



Annual flood sensitivities to El Niño–Southern Oscillation at the global scale

P. J. Ward^{1,2}, S. Eisner³, M. Flörke³, M. D. Dettinger^{4,5}, and M. Kummu⁶

¹Institute for Environmental Studies (IVM), VU University Amsterdam, the Netherlands

²Amsterdam Global Change Institute (AGCI), VU University Amsterdam, the Netherlands

³Center for Environmental Systems Research, University of Kassel, Germany

⁴United States Geological Survey (USGS), La Jolla, CA, USA

⁵Scripps Institution of Oceanography, La Jolla, CA, USA

⁶Water & Development Research Group, Aalto University, Espoo, Finland

Correspondence to: P. J. Ward (philip.ward@ivm.vu.nl)

Received: 17 July 2013 – Published in Hydrol. Earth Syst. Sci. Discuss.: 9 August 2013

Revised: 26 November 2013 – Accepted: 27 November 2013 – Published: 6 January 2014

Abstract. Floods are amongst the most dangerous natural hazards in terms of economic damage. Whilst a growing number of studies have examined how river floods are influenced by climate change, the role of natural modes of interannual climate variability remains poorly understood. We present the first global assessment of the influence of El Niño–Southern Oscillation (ENSO) on annual river floods, defined here as the peak daily discharge in a given year. The analysis was carried out by simulating daily gridded discharges using the WaterGAP model (Water – a Global Assessment and Prognosis), and examining statistical relationships between these discharges and ENSO indices. We found that, over the period 1958–2000, ENSO exerted a significant influence on annual floods in river basins covering over a third of the world’s land surface, and that its influence on annual floods has been much greater than its influence on average flows. We show that there are more areas in which annual floods intensify with La Niña and decline with El Niño than vice versa. However, we also found that in many regions the strength of the relationships between ENSO and annual floods have been non-stationary, with either strengthening or weakening trends during the study period. We discuss the implications of these findings for science and management. Given the strong relationships between ENSO and annual floods, we suggest that more research is needed to assess relationships between ENSO and flood impacts (e.g. loss of lives or economic damage). Moreover, we suggest that in those regions where useful relationships exist, this

information could be combined with ongoing advances in ENSO prediction research, in order to provide year-to-year probabilistic flood risk forecasts.

1 Introduction

Floods are one of the most destructive natural hazards in terms of economic damage, causing billions of dollars of damage each year (Munich Re, 2012), and global flood damages have risen steeply over the past half century (UNISDR, 2011). At the same time, floods are essential for many wetland ecosystems and agricultural practices (Costanza et al., 1997). Hence, improvements in our understanding of global-scale flood processes are generally beneficial.

In recent decades, a large number of studies have examined instrumental discharge records to identify possible changes in flood frequency and/or magnitude due to climate change at national to continental scales (e.g. Allamano et al., 2009; Conway et al., 2009; Cunderlik and Ouarda, 2009; Di Baldassarre et al., 2010; Douglas et al., 2000; Hannaford and Marsh, 2008; Hirsch and Ryberg, 2012; Mudelsee et al., 2003; Shiklomanov et al., 2007; Villarini et al., 2009; Villarini and Smith, 2010), with many more studies than can be listed here focusing at basin scales. There is also a growing literature on possible changes in flood frequency and/or magnitude based on future hydrological projections. Studies at the continental scale (Dankers and Feyen, 2008, 2009;

Feyen et al., 2012; Kitoh et al., 2011; Lehner et al., 2006) to global scale (Hirabayashi et al., 2008, 2013; Milly et al., 2002; Ward et al., 2013) show differing signals of potential change across regions and between models and/or scenarios. Specific studies at the local to national scale are too numerous to be listed here, but are summarised in past reports of the Intergovernmental Panel on Climate Change (IPCC), including the Fourth Assessment Report (Kundzewicz et al., 2007) and the Special Report on Extremes (IPCC, 2012).

Despite this broad research attention to the possible influences of climate change on floods, there has been relatively little attention to the role of present-day interannual climate variability. As a result, the influence of this aspect on flooding is poorly understood, despite its importance for development and adaptation planning (IPCC, 2012). In this paper, we provide the first global assessment of the influences of El Niño–Southern Oscillation (ENSO)-driven climate variations on annual river floods, defined here as the peak daily discharge in a given year. It should be noted that not all annual floods are large or severe; i.e. the annual flood discharge, defined thusly, does not necessarily lead to inundation outside the river channel in all years. We choose ENSO because it is the most dominant interannual climate signal on Earth (McPhaden et al., 2006).

Many past studies have assessed ENSO's impacts on average river flows at the local to basin scale (see, for example, Dettinger et al., 2000, and references therein). Since many of these studies were carried out in regions known to be sensitive to ENSO, many have found significant correlations between average river flows and various indices of ENSO. A few studies have examined global-scale relationships between ENSO and average river flows (Chiew and McMahon, 2002; Dettinger and Diaz, 2000; Dettinger et al., 2000; Labat, 2010), based on discharge measurements from gauging stations, and have found significant relationships in many regions. In contrast, only a few studies have examined relationships between ENSO and peak flows. Most of these studies have focused on the United States (e.g. Bell and Janowiak, 1995; Cayan and Webb, 1992; Cayan et al., 1999), although studies have also been carried out in northern Peru (Waylen and Caviedes, 1986), southern Asia (Mirza, 2011), and the Mekong Basin (Räsänen and Kummu, 2013). To a large extent, the lack of observed daily discharge data in many regions has hampered the kinds of consistent global-scale assessments that are needed. Ward et al. (2010) examined the relationship between ENSO and observed annual peak discharge for 622 gauging stations, but the geographical coverage of those stations was highly biased towards a few regions (particularly North America and central Europe), and for many regions data were limited or lacking.

In this paper, we address this problem by simulating daily discharges using a global hydrological model, allowing for the first fully global assessment of ENSO-driven climate variability's influence on annual floods. We then dis-

cuss key implications of the results for water management and practice.

2 Methods

In brief, we modelled global daily discharges using a global hydrological model forced by daily meteorological re-analysis data. We then identified statistical relationships between annual floods and indices of ENSO. In the following paragraphs, our methods are described in detail.

2.1 Simulating daily discharge

We simulated global gridded daily discharge at a spatial resolution of $0.5^\circ \times 0.5^\circ$ using the WaterGAP model (Alcamo et al., 2003; Döll et al., 2003), forced by daily meteorological fields (precipitation, temperature, and global radiation) for 1958–2000 from the EU WATCH project (Weedon et al., 2011).

WaterGAP consists of two main components: (1) a water-balance model to simulate characteristic macro-scale behaviours of the terrestrial water cycle in order to estimate water availability, and (2) a water-use model to estimate water withdrawals and consumptive water uses. In principle, WaterGAP can account for human influences on the terrestrial water cycle by its inclusion of flow regulation by large dams and reservoirs as well as water withdrawals. For model validation, we used simulations that included these human influences on river discharge. However, as the main focus of this study is climate-induced variability of river floods, we based the present assessment of ENSO influences on naturalised-flow simulations; i.e. human interferences were excluded.

The climate data used to force WaterGAP in this study were obtained from the EU project WATCH (Weedon et al., 2011). WATCH developed a global dataset of sub-daily meteorological forcing data for the period 1958–2001 at a horizontal resolution of $0.5^\circ \times 0.5^\circ$ (WATCH forcing data; WFD). The time series were derived from the ERA-40 reanalysis product (Uppala et al., 2005) via sequential interpolation to a horizontal resolution of $0.5^\circ \times 0.5^\circ$, with elevation corrections and monthly-scale adjustments of daily values to reflect CRU (corrected temperature, diurnal temperature range, cloud cover) and GPCC (precipitation) monthly observations combined with new corrections for varying atmospheric aerosol loading and separate precipitation gauge corrections for rainfall and snowfall derived from the ERA-40 reanalysis product. Full details of the forcing data can be found in Weedon et al. (2011). WATCH also developed time series of the WFD for the period 1901–1957, but these were developed by re-ordering of the ERA-40 data for the later 1958–2001 period. Hence, the extremes in the pre-1958 dataset do not correspond to the extremes in actual years, which is essential for our research. Therefore, in this paper, we used data only from 1958 onwards. The storage

compartments were initialised by re-running the first year of simulation (1958) ten times. This is different to the protocol used in the Water Model Intercomparison Project (WaterMIP; see <http://www.eu-watch.org/watermip>), and was chosen in order to maximise the number of years potentially available for the correlation analyses.

While discharges were simulated on the grid scale, analyses were carried out at basin scales; i.e. correlations with ENSO and other calculations were based on values at the cells farthest downstream in each basin. We present the results at this scale because errors in upstream areas containing just one or a small number of grid cells may be large, particularly due to the use of coarse forcing climate data. Results are thus presented for 11 558 drainage basins. Those basins with an area larger than 750 000 km² were split into sub-basins to show a greater degree of spatial variability there. This means that 34 basins, which drain approximately 40 % of the global land surface area (excluding Antarctica) were divided into 137 sub-basins.

2.2 Calculating mean and maximum annual discharges

For each grid cell and hydrological year, we calculated the maximum annual discharge, or annual flood discharge (Q_{\max}), and the mean annual discharge (Q_{ann}) from the simulated daily discharge time series for hydrological years 1959–2000 (whereby hydrological years are referred to by the year in which they end, as per standard convention). In most cases, we used the standard hydrological year (October–September), as also used in several other global assessments (Dettinger et al., 2000; Dettinger and Diaz, 2000; Ward et al., 2010). However, this is problematic for the allocation of the maximum annual discharge to a given hydrological year for those areas in which that maximum occurs around the boreal autumn (September–November). Therefore, for the most downstream cell of each drainage basin, we calculated the month in which the maximum annual discharge occurred. For those basins in which the maximum annual discharge in the most downstream cell occurred in September, October, or November, we defined the hydrological year as July to June. A map showing the hydrological year used for each basin can be found in Fig. A1 (Appendix A). We also tested the sensitivity of the results to the choice of the months for the alternative hydrological year. To do this, we also used April to March (instead of July–June) as the alternative hydrological year. The differences in the correlation and sensitivity results were found to be minimal in most regions, with some small difference in hyper-arid regions (such as western parts of the western Sahara), where the month of peak discharge is variable.

2.3 Relationships between discharge and ENSO

The time series of annual flood discharges and mean-annual discharges were validated against observed discharge time

series (Sect. 3). We then examined the correlation between the natural logarithm of Q_{\max} ($\ln Q_{\max}$) (and $\ln Q_{\text{ann}}$) and the Southern Oscillation Index (SOI; <http://www.cru.uea.ac.uk/cru/data/soi.htm>), as well as their sensitivities (β_1) to variations in SOI, fitting (Bouwer et al., 2008):

$$\ln(Q_i) = \beta_0 + \beta_1 a_i + \varepsilon_i, \quad (1)$$

whereby Q_i is the simulated Q_{\max} (or Q_{ann}) in hydrological year i , a_i is the 3-monthly mean value of the SOI (OND, NDJ, DJF, JFM), β_0 and β_1 are regression-derived coefficients, and ε_i is an error term. From this, it follows that a unit change in SOI (a_i) is associated with an average increase of 100% ($\exp(\beta_1)-1$) in Q (Q_{\max} or Q_{ann}); we refer to this as the “sensitivity”. In the analyses, the correlations and sensitivity were estimated between $\ln Q_{\max}$ (and $\ln Q_{\text{ann}}$) time series and each of the three-monthly mean SOI values (OND, NDJ, DJF, JFM) separately. We also assessed the three-month period of SOI values with the highest correlation coefficient. To assess the robustness of the results when using other indices of ENSO than SOI, we also repeated the analyses with the negative of the Multivariate ENSO Index (<http://www.esrl.noaa.gov/psd/enso/mei/>), negative NINO3.4 index (<http://www.cpc.ncep.noaa.gov/data/indices/>), and negative Global Sea-Surface Temperature (SST) ENSO index (http://www.jisao.washington.edu/data_sets/globalssstenso/), where negatives were used to accommodate the difference in sign between SOI and SST-based ENSO indices.

The correlations between Q_{\max} and SOI, and between Q_{ann} and SOI, were carried out using the natural logarithms (\ln) of Q_{\max} and Q_{ann} , because the log discharge data are normally distributed for basins covering around 90 % of land surfaces. Normality was assessed using the Lilliefors test; $\alpha = 0.05$. For the vast majority of the other basins, the data were not highly skewed. We primarily assessed the correlations using Pearson’s r , given its greater power over non-parametric equivalents. For verification, we also examined correlations between the original Q_{\max} and Q_{ann} data (not the natural logarithms) using the non-parametric Spearman’s rank test, and found the results to be similar. The normality of SOI data was assessed using the Lilliefors test ($p = 0.24$).

We also examined the percentage anomalies in median Q_{\max} between El Niño (and, separately, La Niña) years compared to the median Q_{\max} of all years. We used the classification of ENSO years from the Center for Ocean-Atmospheric Prediction Studies (<http://coaps.fsu.edu/jma.shtml>), as shown in Table 1. The non-logarithmic Q_{\max} time series used in this composite analysis are only normally distributed in basins covering 50 % of the land surfaces. Therefore, when assessing differences in Q_{\max} between El Niño (La Niña) and all years, we used the non-parametric Mann–Whitney U test to assess the statistical difference in median values.

Table 1. Hydrological years categorised as El Niño and La Niña, based on the ENSO classification of the Center for Ocean-Atmospheric Prediction Studies (COAPS) of Florida State University (<http://coaps.fsu.edu/jma.shtml>).

ENSO mode	Hydrological year
El Niño	1964, 1966, 1970, 1973, 1977, 1983, 1987, 1988, 1992, 1998
La Niña	1965, 1968, 1971, 1972, 1974, 1975, 1976, 1989, 1999, 2000

3 Validation

The general ability of global hydrological and land surface models, including WaterGAP, to reproduce various spatial and temporal characteristics of 20th-century river discharge, using the WFD forcing data, has been evaluated extensively by the WATCH project. Those analyses evaluated model performance for long-term mean runoff (Haddeland et al., 2011), as well as high- and low-flow indices (Gudmundsson et al., 2011; Prudhomme et al., 2011). WaterGAP was found to acceptably reproduce most regional characteristics of large-scale hydrological extremes.

However, these validations did not specifically assess the model's performance in simulating differences in peak discharges between different phases of ENSO. Thus, in this study we validated model findings against observed discharge time series from the GRDC database, using only those stations with upstream areas greater than 10 000 km² for which daily data are available for every day of the hydrological year in at least 15 hydrological years between 1959 and 2000. This yielded a set of 721 observed discharge time series. For model validation, we used WaterGAP simulations including human influence.

From Fig. 1, it is clear that there are large biases between modelled and observed Q_{\max} for many stations. At 33 % of the stations, the percentage difference between modelled and observed median Q_{\max} is less than 25 % (positive or negative), but large positive biases (> 50 %) were found for 24 % of stations, and large negative biases for 15 %.

For this study, though, we are most interested in the relative change in discharge magnitudes from year to year, and between different phases of ENSO, rather than absolute discharge values. In Fig. 2, we show that the correlation between modelled and observed $\ln Q_{\max}$ is generally good. For 58 % of stations, the correlation coefficient (r) is greater than 0.6, and greater than 0.4 for 81 % of stations. We also carried out correlation analyses using the non-parametric Spearman's rank correlation coefficient (not shown here), using the original Q_{\max} data (instead of the natural logarithms), and found very similar values. Moreover, the majority of the stations with low correlation are located in upstream areas, whereas the analyses presented in this paper are based on values at the most downstream cell in each basin. This gives

confidence that the model simulates interannual fluctuations in Q_{\max} similar to those in the observed records.

Finally, we examined the agreement between the modelled and observed data in terms of the relative change in Q_{\max} between El Niño and non-El Niño years (Fig. 3a) and between La Niña and non-La Niña years (Fig. 3b). For 90 % (92 %) of the stations, both modelled and observed median Q_{\max} show either no significant difference between El Niño (La Niña) and non-El Niño (non-La Niña) years, or significant differences of the same sign. For the other stations there was a statistically significant difference in modelled median Q_{\max} between El Niño (La Niña) and non-El Niño (non-La Niña) years, but none for observed data (or vice versa). Finally, there are no stations at which modelled and observed median Q_{\max} show significant changes between El Niño and non-El Niño years or between La Niña and non-La Niña years with different signs.

4 Results and discussion

In this section, we first show and discuss the relationships between annual floods and ENSO at global and regional scales, and then examine how these relationships have changed over time. We also show and discuss the anomalies of annual flood discharge associated with the two ENSO phases, and relate our findings to past research based on observed discharge time-series. Finally, we discuss the implications of our results, the main limitations of our study, and suggestions for future research. Although all of our analyses were originally carried out at the grid-cell level, we display results by hydrological basin, based on relationships to discharges at the most downstream cell. Throughout the text, the analyses are based on naturalised flows; i.e. the simulations do not include human influences on discharge.

4.1 Global sensitivity of flood discharge to ENSO

To the best of our knowledge, Fig. 4 is the first spatially explicit fully global representation of the sensitivity of annual flood discharge (Q_{\max}) to ENSO. The figure shows the sensitivity of $\ln Q_{\max}$ to 3-monthly averages of the SOI (OND, NDJ, DJF, JFM), where at each site the sensitivity shown is for the 3-monthly period of the SOI most highly correlated to the annual floods. We chose to do this because it gives more information on the correlations than simply one fixed 3-month period; the rest of the results in Sects. 4.1 and 4.2 are also based on these data. However, in Fig. A2 we show the same results, but for each 3-month period separately (i.e. OND, NDJ, DJF, JFM). The latter figure shows that the sensitivities are generally similar between the periods OND, NDJ, and DJF, but the strength of the correlations has begun to break down in the majority of regions by JFM. Sensitivities to SOI during boreal-winter seasons are analysed because

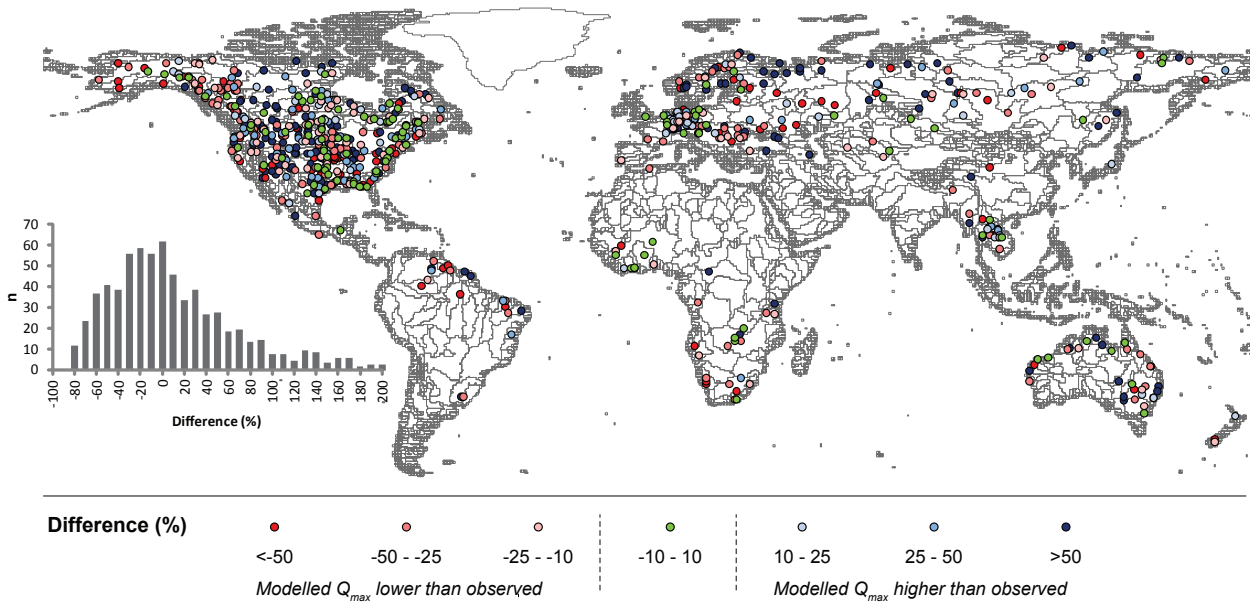


Fig. 1. Percentage difference between modelled and observed median Q_{max} over the period 1959–2000. Inset shows histogram of values for individual locations (difference > 200 % for 58 locations).

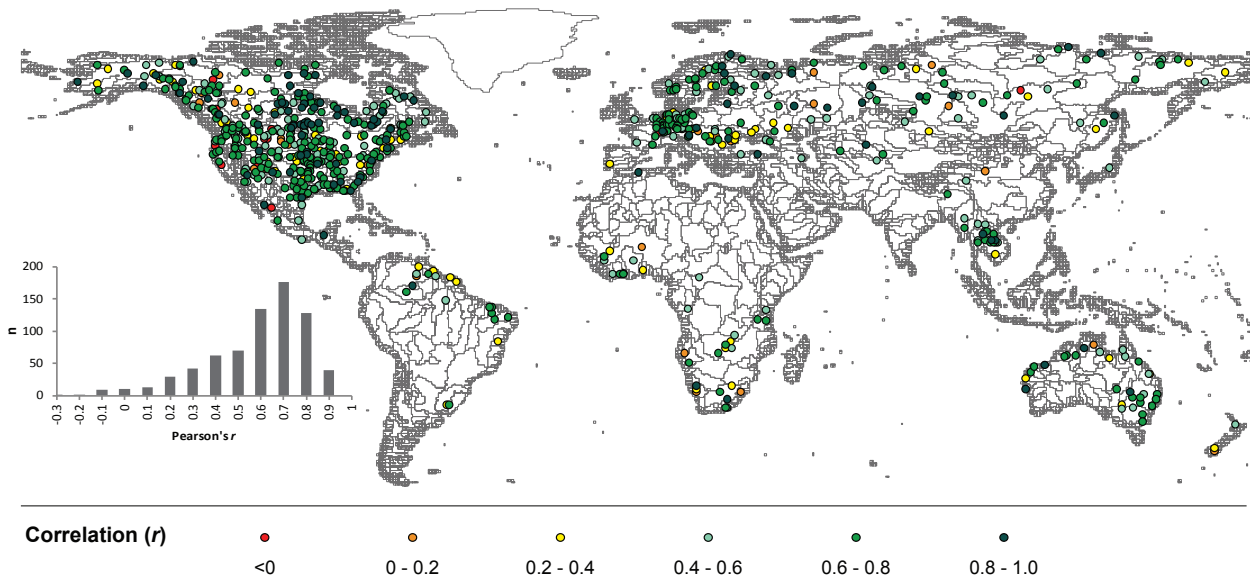


Fig. 2. Correlation (r) between modelled and observed $\ln Q_{max}$ time series over the period 1959–2000. Inset shows histogram of values for individual locations. The median value of r is 0.64, and the 25th and 75th percentiles are 0.48 and 0.75, respectively.

this is the season in which ENSO reaches its fullest tropical expression (Neelin et al., 2000).

In Fig. 4, the sensitivity results are shown for basins in which the correlation reaches statistical significance at a 10 % confidence interval ($\alpha = 0.10$). At locations for which observed daily discharge time series were available in the study of Ward et al. (2010), the results in Fig. 4 are very similar to that study. This further supports the use of the modelled data for assessing the influence of ENSO on annual flood dis-

charges. Since the choice of the confidence interval is subjective, we also present the results using a confidence interval of 5 % ($\alpha = 0.05$) in Fig. A3, and sensitivity results for all basins without significance testing in Fig. A4. Generally, we find the same overall regional patterns when the 5 and 10 % confidences are used, though evidently the number of basins with significant correlations is lower in the former, particularly for many of the very small single-cell coastal basins.

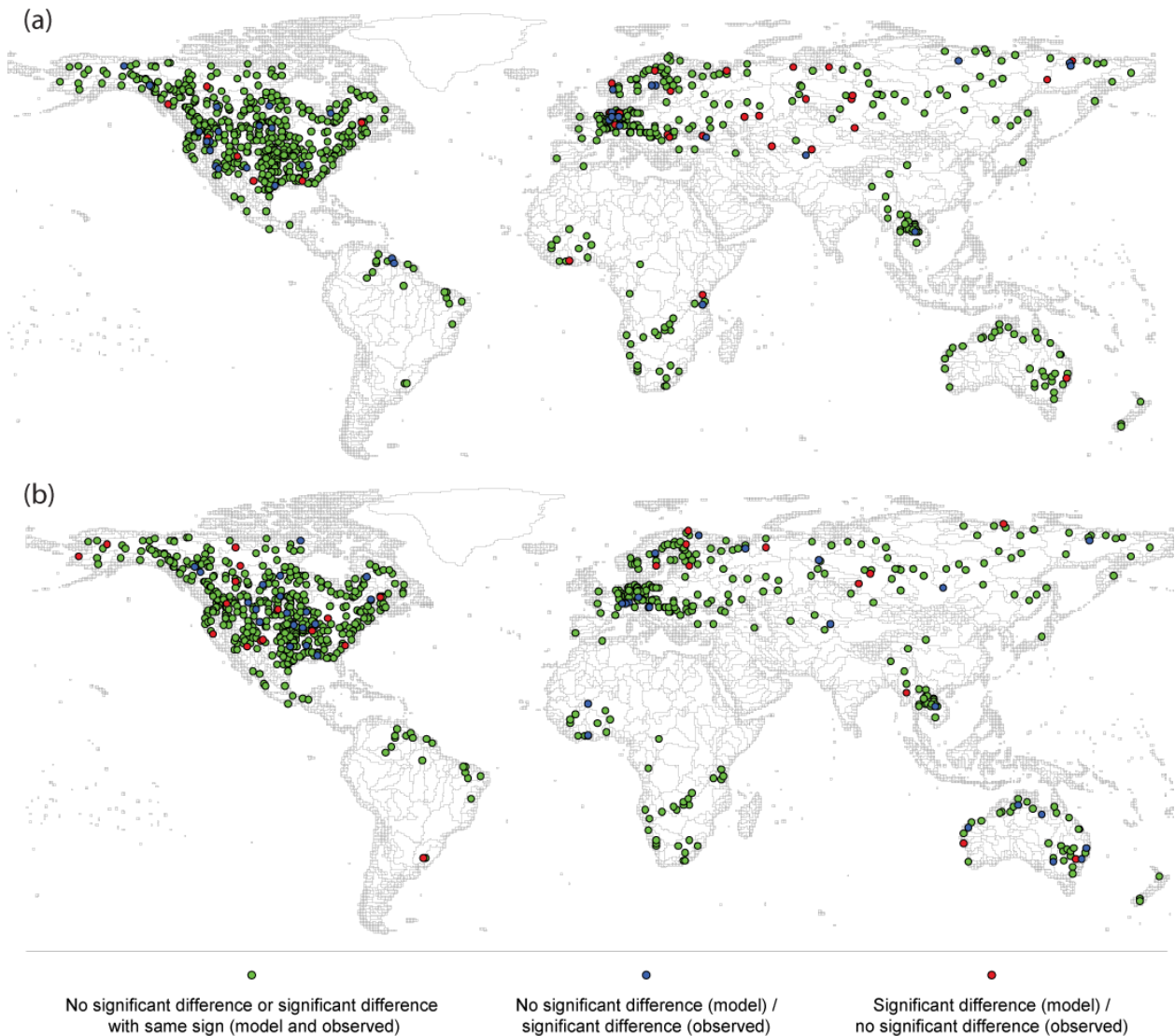


Fig. 3. Indicator of the agreement/disagreement between modelled and observed median Q_{\max} between (a) El Niño years and non-El Niño years, and (b) La Niña years and non-La Niña years. There are no stations for which modelled and observed median Q_{\max} show significant differences between El Niño and non-El Niño (or La Niña and non-La Niña years) years with the opposite sign. Statistical significance was assessed using a 2-tailed Mann–Whitney U (MWU) test; $\alpha = 0.05$.

We also assessed how robust the correlations are to the selected ENSO index, by examining the correlations with three other indices of ENSO (negative of Multivariate ENSO Index, negative of NINO3.4 index, and negative of Global SST ENSO index). Those results are shown in Fig. A5, indicating broadly similar patterns among correlations to the four indices. In the rest of this paper, we focus on SOI, since this allows for direct comparison with past studies (Chiew and McMahon, 2002; Dettinger and Diaz, 2000; Dettinger et al., 2000; Ward et al., 2010) and may allow for somewhat greater predictability (Redmond and Koch, 1991).

We found significant correlations between SOI and $\ln Q_{\max}$ ($\alpha < 0.10$) for basins covering over a third (37%)

of land surfaces (Fig. 4). These correlations are positive for basins covering 23% of land surfaces, and negative for basins covering 14% of land surfaces. In other words, there are more land areas where Q_{\max} increases with La Niña and decreases with El Niño conditions than vice versa. This finding is important, since past studies examining relationships between the impacts of flood disasters and ENSO at the global scale have tended to only focus on El Niño episodes, and not La Niña. For example, two studies of the relationship between ENSO and the frequency of major floods around the globe (Dilley and Heyman, 1995; Goddard and Dilley, 2005) found no differences between El Niño and non-El Niño years, but La Niña years were not evaluated. Similarly,

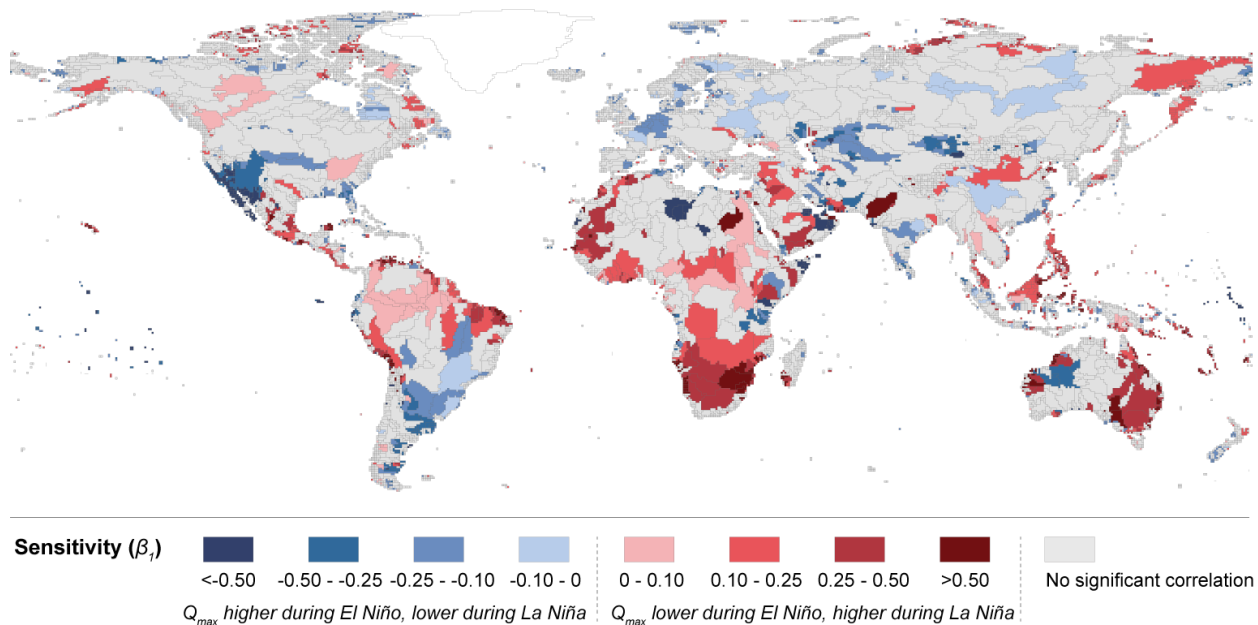


Fig. 4. Sensitivity (β_1) of $\ln Q_{\max}$ to variations in SOI. Sensitivity is only shown for basins with significant correlation at a 10 % confidence interval (Pearson’s r , t statistic, $\alpha = 0.10$). Negative correlation generally represents higher annual floods in El Niño years/lower annual floods in La Niña years, while positive correlation generally represents lower annual floods in El Niño years/higher annual floods in La Niña years.

another study of the number of people affected by natural hazards also only examined differences between El Niño and non-El Niño years (finding strong relationships), but did not examine La Niña years (Bouma et al., 1997). Whilst the results here only show that annual floods (which span a large range of magnitudes) are correlated with ENSO, the relationships suggest that there may also be significant links between ENSO and floods large enough to lead to flood disasters. Indeed, fitting extreme value distributions to the annual flood series leads to significantly different estimates of extreme floods when either El Niño or La Niña years are dropped from the time series (not shown here).

We also found that Q_{\max} is more sensitive to changes in SOI than is Q_{ann} in basins covering the majority (76 %) of the Earth’s land surface (Fig. 5), with sensitivity results for Q_{ann} shown in Fig. A6. If we only consider basins in which the correlation between Q_{\max} and SOI is statistically significant, the sensitivity of Q_{\max} is greater than that of Q_{ann} for basins covering 32 % of land areas, whilst Q_{ann} is more sensitive for basins covering 4 % of land areas. If we only consider basins in which the correlation between Q_{ann} and SOI is statistically significant, the sensitivity of Q_{\max} is greater than that of Q_{ann} for basins covering 31 % of land areas, whilst Q_{ann} is more sensitive for basins covering 16 % of land areas. In earlier work based on observed discharges at 622 gauging stations, Ward et al. (2010) also found that, on average, ENSO has a greater impact on annual flood discharges than on mean discharges. Similarly, for observed discharges in the west-

ern USA, Cayan et al. (1999) found ENSO to have a greater impact on the number of days exceeding the 90th percentile values of streamflow as compared to the number of days exceeding the 50th percentile (i.e. median) values. In Europe, Bouwer et al. (2008) also found annual peak discharge to be more sensitive than annual mean discharge to variability in various large-scale atmospheric circulation patterns. Research is now required to examine the mechanisms behind these apparent differences in the sensitivity of peak and mean discharges to large-scale atmospheric circulation.

4.2 Regional sensitivities of flood discharges to ENSO

There are several regions in which it is common knowledge that climate is affected by ENSO through teleconnections (Kiladis and Diaz, 1989), for example eastern Australia, southeastern Asia, parts of western South America, and western North America. However, little is known on the influence of ENSO teleconnections on annual floods at these large regional scales. In Table 2, we show the area-weighted percentage differences (unsigned) in Q_{\max} per unit change in SOI, per geographical region (Kummu et al., 2010) and Köppen climate zone (Kottek et al., 2006), for those basins where the correlations in Fig. 4 are significant. We also present the percentage of land in each region/zone combination for which the correlations are significant. Globally, in those basins with significant correlation (i.e. basins covering 37 % of global land surface), Q_{\max} varies by 27 % for each unit change in SOI: this includes regions far removed from the classic

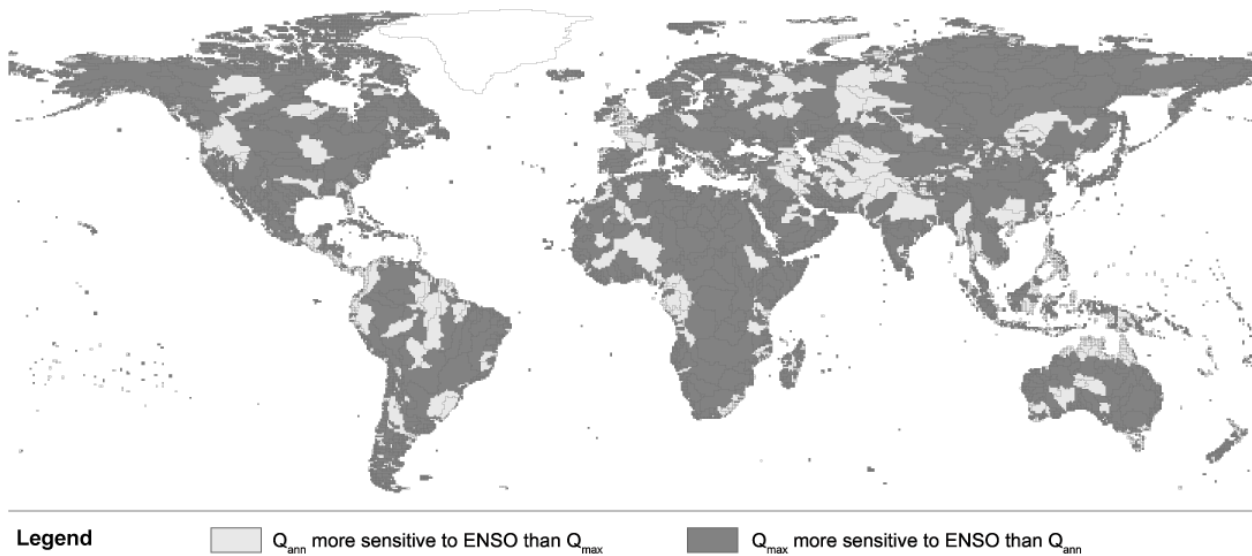


Fig. 5. Basins in which Q_{max} (Q_{ann}) is more sensitive than Q_{ann} (Q_{max}) to changes in SOI and vice versa.

Table 2. Sensitivity of annual flood discharge to SOI*.

	Percentage change in Q_{max} per unit change SOI (land area, %)				
	Equatorial	Arid	Warm temperate	Cold**	All Köppen zones
Australia and Oceania	36 % (43 %)	63 % (45 %)	28 % (29 %)	16 % (23 %)	45 % (39 %)
Central America	29 % (41 %)	98 % (62 %)	26 % (21 %)	N/A	54 % (46 %)
Eastern Asia	N/A	31 % (18 %)	11 % (51 %)	21 % (10 %)	16 % (29 %)
Eastern Europe & central Asia	N/A	24 % (33 %)	15 % (12 %)	11 % (22 %)	14 % (23 %)
Indian Subcontinent	15 % (45 %)	63 % (30 %)	N/A	N/A	35 % (26 %)
Latin America	14 % (53 %)	49 % (27 %)	16 % (82 %)	205 % (25 %)	17 % (54 %)
Middle East	N/A	42 % (40 %)	11 % (12 %)	13 % (72 %)	40 % (38 %)
Middle and southern Africa	21 % (55 %)	52 % (49 %)	64 % (17 %)	N/A	35 % (51 %)
Northern Africa	5 % (73 %)	39 % (38 %)	25 % (34 %)	N/A	32 % (41 %)
North America	N/A	50 % (55 %)	17 % (32 %)	11 % (19 %)	19 % (25 %)
Southeastern Asia	20 % (37 %)	N/A	8 % (37 %)	N/A	18 % (37 %)
Western Europe	N/A	N/A	13 % (28 %)	11 % (27 %)	13 % (28 %)
All regions	19 % (50 %)	49 % (40 %)	16 % (37 %)	12 % (21 %)	27 % (37 %)

* Area-weighted percentage change in Q_{max} per unit change SOI for basins with significant correlations between $\ln Q_{\text{max}}$ and SOI, and percentage of land area (shown in brackets) with significant correlations. Results shown per geographical region and Köppen climate region. ** Köppen regions “polar” and “snow” have been combined here into one ‘cold’ region. Greenland and Antarctica are excluded from the analysis.

ENSO regions named above. In equatorial regions, Q_{max} is significantly correlated with SOI in basins covering half of the land areas.

The highest sensitivities are found in arid regions, followed by equatorial regions. The sensitivity of discharge to ENSO in tropical regions has been widely reported (e.g. Dettinger and Diaz, 2000; Dettinger et al., 2001; Ward et al., 2010), since ENSO affects climate in tropical regions through perturbations in the Walker circulation (Kiladis and Diaz, 1989). However, less research has assessed the influence of ENSO on the hydroclimatology in arid regions. Whilst the paucity of observed discharge data in many of

these regions limits the validation of our model results there, the strength of the signal provides motivations for enhancing research activities in those regions, in order to examine whether this is related to physical processes, and if so which, and/or whether this is related to the high coefficient of variability in peak flows. This is especially the case since many arid regions of the developing world are expected to show some of the world’s largest increases in population and asset values in coming years (Jongman et al., 2012).

One arid region in which there are good records of discharge, and an abundance of studies on ENSO and hydroclimatology, is the southwestern USA. Here, several studies

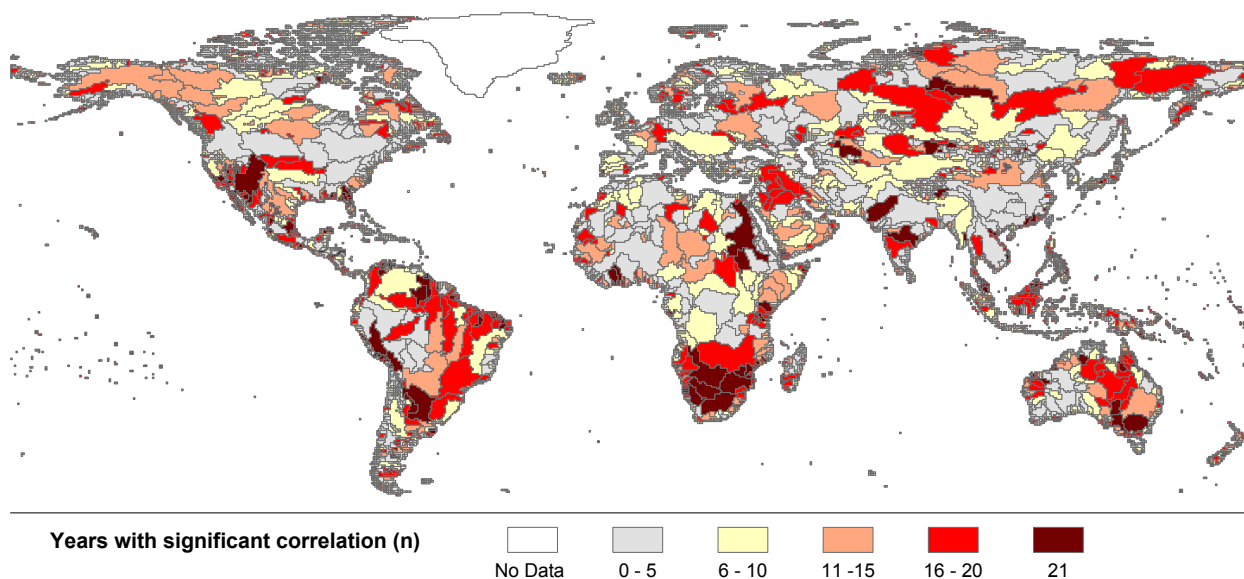


Fig. 6. Number of years (n) for which the correlation (Pearson's r) between $\ln Q_{\max}$ and SOI_{DJF} is statistically significant ($\alpha = 0.10$), based on 21 yr moving windows centred on 1969 to 1989.

have indeed found strong relationships between ENSO and annual or seasonal discharge (e.g. Hidalgo and Dracup, 2003; Piechota et al., 1997) or between ENSO and drought conditions (Piechota and Dracup, 1996). Generally, these studies found wetter conditions in El Niño years and drier conditions in La Niña years. Cayan and Webb (1992) and Cayan et al. (1999) also found relationships between ENSO and extreme discharges at a large number of locations in the arid regions of southwestern USA, with high-flow conditions being more likely in El Niño years (see Sect. 4.4 for details).

In terms of geographic regions, the highest sensitivities of annual floods to ENSO are found in Central America (54 %) and the lowest in western Europe (13 %), with large differences between climatic zones in the geographical regions. For example, floods in the equatorial zone of Australia and Oceania are far more sensitive than in the equatorial zone of northern Africa. Moreover, the sensitivity is particularly high in several less developed regions (e.g. Africa, Indian Subcontinent, Central America) compared to highly developed regions (western Europe, North America), although this does not hold for all cases (for example, sensitivity is also high in Australia and Oceania). Brown and Lall (2006) found significant correlation between the coefficient of variation of rainfall variability and per capita GDP at the country scale, and it might be useful to evaluate similar relationships between ENSO-driven hydrological variability and GDP or other development indicators.

4.3 Changes in ENSO–flood relationships through time

Whilst we have shown significant correlations between SOI and annual floods for the overall 1959–2000 period, it is

known that the strength of ENSO has changed over time on timescales from millennia to decades (e.g. Cane, 2005; Li et al., 2013; Mann et al., 2005; McPhaden et al., 2006; Tudhope et al., 2001; Wunsch, 1999) and that its teleconnected influences to at least some distant regions (e.g. western North America and South America) have likewise varied (Gershunov and Barnett, 1998; Gershunov et al., 1999; McCabe Jr. and Dettinger, 1999; Dettinger et al., 2000). Hence, we examined whether we could find any indication of changes in the strength of the correlation between annual floods and ENSO through time. To do this, we assessed changes in the strength of the correlation between SOI_{DJF} (i.e. the mean SOI value for the months of December, January, and February) and $\ln Q_{\max}$ using a 21 yr moving window, ranging from 1959–1979 to 1979–1999. A 21 yr moving window was used as a trade-off to maximise both the number of years per window (21) and the number of windows (21), but the relevance of this decision was tested separately, as outlined below. DJF was chosen since the correlations are strongest for this 3-month period for the largest number of basins. In Fig. 6, we map the numbers of windows for which the flood–SOI correlations within the 21 yr windows are statistically significant (Pearson's r , $\alpha = 0.10$). This figure gives an indication of the temporal stationarity (and thus long-term reliability) of the correlation between SOI and annual floods by river basin. In those basins shown in the darkest shade of red, 21 yr correlations are statistically significant throughout the 1959–2000 era. Basins with the most persistent or reliable correlations are found in southern Africa, several parts of South America, eastern Australia, the southwestern USA, the Nile basin, northern India, and several basins in central and northern Asia.

In Fig. 7, we show how the strength of this correlation has changed over the period 1969–1989 (again based on the 21 yr moving windows described above, whereby 1969–1989 are the central years of the moving windows) for selected basins. We also show whether there are significant linear trends in the strength of the correlations (“no trend”; correlations growing “stronger” over time; or correlations growing “weaker” over time), based on the Mann–Kendall test ($\alpha = 0.10$). The analyses were carried out for the 50 largest basins for which correlation over the entire period 1959–2000 proved significant. In order to make the figure clearer, we then removed several upstream sub-basins (e.g. several Amazon tributaries) where the overall signal was similar to that at the most downstream sub-basin.

Several interesting regional patterns can be seen in Fig. 7. In South America, it appears that the strength of correlations between ENSO and flood discharges have strengthened over the period of analysis here in basins from Brazil southwards, except for the Tocantins. On the other hand, in northern South America, the strength of the correlation has weakened in the Essequibo, with no significant trend in the Magdalena. In North America, correlations for the Ohio and Lower Missouri (both tributaries of the Mississippi) have strengthened, albeit as an increasingly positive correlation in the former and an increasingly negative correlation in the latter. The results for the Colorado show no significant trend over the study period. The only basin shown here in North America for which the strength of the correlation weakened significantly is the Fraser River.

For basins in western and north-central Eurasia, we found either weakening correlations or no significant trends. For both the Yenisei and the Rhine, we found fairly strong negative correlations until the 21 yr period centred on ca. 1981, and much weaker correlation thereafter (reaching zero for 21 yr periods centred after 1997 in the case of the Rhine). In southern Asia, the two basins shown both exhibit weakening correlations. On the other hand, the basins shown in eastern Asia (Chao Phraya, Yellow, Kolyma) all show trends of strengthening positive correlations over time. For the basins shown in Australia and Africa, a highly mixed picture in terms of trends emerges; however, it should be noted that the strength of the correlations remains rather strong in the majority of these basins throughout the study period.

On the whole, of the 35 basins highlighted in Fig. 7, correlations strengthened in 14 basins, weakened in 13, and exhibited no trend in 8. Thus, globally, there has been essentially no overall bias among the changing teleconnections in one direction or the other. This even global mix of strengthening versus weakening teleconnections may suggest that the changes shown in Figs. 6 and 7 reflect changes in teleconnection strengths, rather than changes in the strength of the driving ENSO variations. The latter may more likely yield more universally consistent changes in flood correlations.

We also repeated the analyses using a 15 yr moving window (which yields 27 windows for the trend detection). The

results of the latter analyses were similar to those using a 21 yr moving window, with the following differences: the Yellow, Murray, and Ohio rivers displayed no significant trend (instead of strengthening), and the Tocantins displayed no significant trend (instead of weakening).

In some regions, these long-term variations in ENSO teleconnections have been recognised in annual precipitation and streamflow records. For example, in the Mekong Räsänen and Kumm (2013) found epochal behaviour in ENSO–discharge correlations, with strongly negative correlations in the pre-1940s and after the mid-1970s, but a rather weak relationship between these periods. Similar results were found by Zubair and Chandimala (2006), who investigated ENSO–seasonal-stream-flow relationships in Sri Lanka, and found that the correlations changed from positive (pre-1950) to strongly negative (post-1970). These findings are supported by other studies, which found similar epochal behaviour in relationship between ENSO and Asian-Australian Monsoon (Wang et al., 2008), and ENSO and Indian Monsoon (Torrence and Webster, 1999). Outside Asia, Beebe and Manga (2004) found that ENSO correlations with snowmelt runoff in Oregon, USA, were weaker between 1920 and 1950 than in periods before and after those decades. Such long-term variations in ENSO teleconnections have been associated with interferences and enhancements from multi-decadal climate modes, for example ENSO interactions or reflections of the Pacific Decadal Oscillation (PDO) as reported by Gershunov and Barnett (1998), Gershunov et al. (1999), and McCabe Jr. and Dettinger (1999). There are many such “low-frequency” modes in the climate system, including also modes in the Atlantic (e.g. Apipattanavis et al., 2009; McCabe Jr. et al., 2004) and Indian Ocean basins (e.g. Hoerling et al., 2009, 2010), so that the particular interferences at work in any given river basin may be complex and likely require more research to identify. Indeed, it is also possible that human-caused multi-decadal climate trends themselves may be modifying some of these teleconnection strengths, or may do so in the future.

4.4 Flood discharge differences between ENSO phases

We also examined the differences in anomalies of annual flood discharge between ENSO phases. Figure 8 shows anomalies of median Q_{\max} in (a) El Niño years compared to all years, and (b) La Niña years compared to all years. In a general sense, the patterns are similar to those shown in Fig. 4. However, this analysis allows us to identify additional conditionalities and relationships that were obscured in the correlation and sensitivity analysis in Sect. 4.1. Here, we can see several regions in which there are asymmetric responses; i.e. there is an anomaly in either El Niño or La Niña years, but not in the opposite. For example, in the Darling basin in eastern Australia Q_{\max} shows an anomaly in excess of +75% in La Niña years, yet there is no (or little) average anomaly (–10% to +10%) during El Niño years; and



Fig. 7. Correlation (Pearson’s r) between $\ln Q_{\max}$ and SOI_{DJF} for 21 yr moving windows centred on the years 1969–1989. On the line graphs, the axes are unlabelled due to space constraints: the x axes show years (1969–1999) and the y axes show the strength of Pearson’s r (+1 to –1). The blue line indicates the strength of the correlation, and the red dashed lines indicate the critical values of the significance test (critical $r = 0.369/-0.369$, $\alpha = 0.10$). The names of the basins are shown in text, as well as the trends in the strength of the correlation over time (no trend; stronger (i.e. strengthening over time); or weaker (i.e. weakening over time)). The significance of the trends was assessed using the Mann–Kendall test ($\alpha = 0.10$). The results are shown for 35 basins, selected as per the description in Sect. 4.3.

the Mekong basin shows an anomaly of -25% in La Niña years, yet no anomaly in El Niño years. On the other hand, there are also basins with anomalies in El Niño years, but no anomaly in La Niña years, for example the Limpopo River in southern Africa. Asymmetries between El Niño and La Niña influences may reflect some complications associated with interferences with multi-decadal climate modes, as discussed earlier, but are also reasonably well known to be direct outgrowths of the overall non-linearities of the climate system (Mullan, 1995; Hoerling et al., 1997). Further research into the driving mechanisms for such asymmetric patterns could advance our understanding of why basins respond differently to hydroclimatic variations.

This El Niño versus La Niña comparative analysis allows us to compare our findings to the limited number of studies in the literature that have also examined such relationships based on observed annual flood discharge. Cayan and Webb (1992) analysed daily discharge data for the Santa Cruz River at Tucson, Arizona, for 1914–1986, and found that the presence of El Niño affects the probability of flooding in a given year. They estimated the magnitude of a 100 yr flood based on the time series of maximum annual discharges with and without the data for El Niño years, and found the results to be a factor two higher when the El Niño data were included. In this region, we found large anomalies in simulated annual flood discharge of about $+50\%$ in El Niño years. Cayan et al. (1999) then examined relationships between SOI and observed river discharge at 303 locations in the entire western USA. They analysed the number of days per year with discharge in excess of the 90th percentile in both El Niño and La Niña years. They found that in El Niño years, days with high daily discharge occur more frequently than average over the southwestern USA and less frequently than average over the northwestern USA, and for La Niña years they found an almost opposite pattern. Although the metric used in our study is different, we find a corresponding pattern of higher (lower) flood discharges in the southwestern USA in El Niño (La Niña) years. In the northwestern USA, for example for the Columbia River, we find strongly higher flood discharge in La Niña years ($+26\%$) and somewhat lower flood discharge in El Niño years (-8%).

Waylen and Caviedes (1986) analysed observed time series of annual floods for 13 rivers in the northern coastal region of Peru. They found that the annual flood is generally higher in El Niño years than in La Niña years, with the greatest anomalies towards the more northern and coastal locations. For this area we found similar results, with significant negative correlations between SOI and $\ln Q_{\max}$ ranging from -0.1 to -0.4 and the highest values in the northern coastal region ($r = -0.3$ to ca -0.4 in this region).

Whilst the results of the above studies based on observed discharges generally corroborate our modelled findings, we did find some differences between our results and the analyses of Räsänen and Kummu (2013) for the Mekong. They examined the correlation between maximum annual discharge

at Strung Teng (a downstream gauging station) and DJF values of the monthly ENSO index developed by Meyers et al. (2007) and later updated by Ummenhofer et al. (2009). Their analyses were carried out for the period 1981–2005, and yielded a correlation of $r = -0.49$. This is higher than the value of $r = -0.106$ that we found in our study for the period 1959–2000. However, it should be noted that our analyses of the change in correlation over time show that the strength of the simulated correlation changed significantly over the period 1969–1989, with values of r ranging from $+0.13$ to -0.27 . The overall trend is towards stronger negative correlations in the later period, which corresponds most closely to the time-period used by Räsänen and Kummu (2013). Also, the two studies are based on a different index of ENSO. Thus the differences between that study and the present analysis may reflect analytical or temporal differences in the data and methodologies used.

Knowledge of these El Niño–La Niña asymmetries can be useful for more precisely targeting (on one ENSO phase or the other, or both) plans and accommodations for the ENSO influences on flood magnitudes and, ultimately, flood risks in individual basins around the world.

4.5 Implications and recommendations

Given our finding that ENSO correlates significantly with annual flood discharge in basins covering over a third of global land surfaces, there is a clear need for more research on the influence of interannual and longer-term climate variability on flood hydrology. This would complement and lend greater practical urgency to ongoing efforts to better understand the roles of ocean–atmosphere interactions on climate more generally, such as that carried out under CLIVAR (Climate Variability and Predictability Programme of the World Climate Research Programme). Specifically, if significant correlations exist between ENSO and even more extreme flood discharges, then the socioeconomic impacts of flooding in some regions may also be related to, and predictable from, ENSO. To examine this, future research may assess the impacts of ENSO directly on flood risk, where risk is a product of the probability of flooding and the consequences of flooding.

Another promising research avenue would be to use the potential predictability of ENSO (Cheng et al., 2011) to provide probabilistic estimates of flood risk with lead times up to several seasons. The coupling of ENSO predictability with hydrometeorological variables such as precipitation and mean discharge has been on the research agenda for over a decade. However, also coupling such analyses with flood statistics and global risk models could provide probabilistic flood risk forecasts, enabling humanitarian and development agencies to prioritise short-term risk reduction efforts in the most at-risk regions. This would enable (re-)insurance companies to accommodate anomalies in their risk portfolios in the coming seasons to years, and potentially enable improved flood early warning and flood regulation by dam operators.

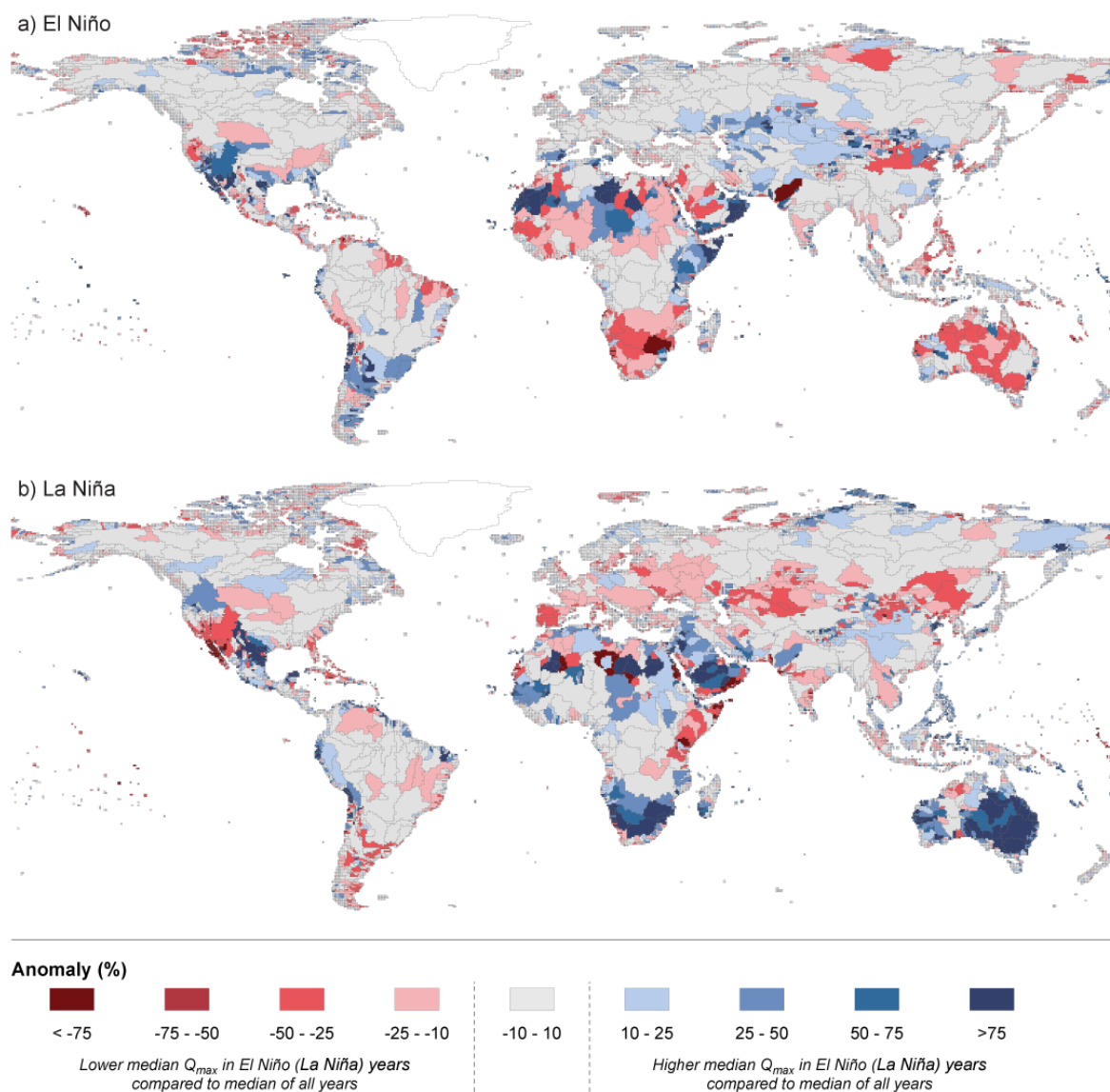


Fig. 8. Anomaly (percentage) in median Q_{\max} between (a) El Niño years and all years, and (b) La Niña years and all years. Positive anomalies indicate higher median Q_{\max} in El Niño (La Niña) years compared to the median of all years, and negative anomalies indicate the opposite.

However, in this study we have shown that the strength of the correlation between ENSO and annual floods is itself non-stationary through time. Hence, such analyses may be more suited to those regions where the temporal persistence of the ENSO–flood correlations is highest.

Technical flood defences are designed to protect against floods with given return periods, estimated from observed discharge records. However, should ENSO magnitude and frequency change over time, as has occurred in the recent and geological past (Mann et al., 1995; McCabe Jr. and Dettinger, 1999), this would result in effective over- or underdesign of flood protection infrastructure, such as dikes, for decades at a time. The present study identifies some areas where this may

be most likely, i.e. those locations where floods are particularly sensitive to changes in ENSO. Notably, recent studies of ENSO variation under climate change have projected enhanced ENSO variability, as well as enhanced ENSO-related precipitation variability, in response to increased tropical energetics and moisture availability in a warming world (IPCC, 2013; Power et al., 2013). Such enhancements may serve to make the ENSO–flood relations identified here all the more forceful and relevant in coming decades.

Along with these extensions of the current research to potentially facilitate flood risk analyses, a number of analytical steps could be improved in future research. Firstly, as stated earlier, the correlations are shown for naturalised flows. In

reality, flood control measures taken in some basins may have affected the strength of the flood peak, and hence the strength of the correlations. An examination of this issue would provide an interesting future research avenue. Future research could also examine the relationships between ENSO and floods using additional climate indices or several different global hydrological models. Also, given the possible interaction between ENSO and other large-scale climate oscillations (such as PDO) that may serve to modulate ENSO relationships with flood discharge, analyses should be carried out using a wide range of interannual ocean–atmosphere interactions, in addition to ENSO. Finally, we recommend that future studies carry out detailed analyses of relationships between Q_{\max} and its climatological forcing to reveal regions in which climate dominates Q_{\max} variability, versus those where this effect may be decreased or amplified by other factors, such as terrain, soil, cropping, or human flow management.

Finally, it is important to note that a global approach provides information on the large-scale regional influences of ENSO on (extreme) discharge, but cannot provide the level of detail for specific basins that can be provided by studies based on local gauged data or hydrological data. Hence, for those regions described in this paper for which studies using such local datasets have already been conducted, the results of those previous studies can provide more detail than this current paper. However, as noted earlier, there are to date very few locations where the influence of ENSO on extreme discharge has been specifically examined. Our paper suggests the opportunity for similar studies at more local scales in those regions identified as being ENSO-sensitive.

5 Conclusions

In this paper, we provide the first fully global assessment of ENSO-driven climate variability's influence on annual floods. This was achieved by simulating daily discharges over the period 1958–2000 using the WaterGAP model forced by global climate reanalysis data from the WATCH project. We first validated the simulated annual flood discharges by comparisons to observed discharges. We found that, whilst there are large biases between modelled and simulated annual floods, they simulate similar relative changes in annual floods from year to year, and that their agreement is good in terms of the signal of change between different phases of ENSO. Whilst studies on the linkages between ENSO and flood discharge based on observations are limited, the findings of the available studies are generally in line with our model results. This adds confidence to our use of modelled data in these analyses.

We found that ENSO has a significant influence on annual floods in river basins covering over a third of the world's land surface, and that its influence on annual floods is much greater than its influence on average flows. This includes re-

lationships in the classic ENSO regions, such as eastern Australia, southeastern Asia, western North America, and parts of western South America, but also areas far beyond. We also found that the strengths of the correlations between ENSO and flood discharge are non-stationary. In some regions, the strength of the relationships increased (e.g. South America, parts of the USA, and eastern Eurasia) over the study period, whilst in others strengths have decreased (e.g. parts of western and north-central Eurasia). Thus, globally, there has been essentially no overall bias among the changing teleconnections in one direction or the other. Such changes may be related to the modulation of the general amplitudes of ENSO. However, given the global mix of strengthening versus weakening teleconnections, this may suggest that the changes reflect changes in teleconnection strengths.

We also found that there are more basins in which annual floods increase with La Niña and decrease with El Niño than vice versa. This is an important finding, since past studies on relationships between ENSO and disaster impacts have only examined differences between the El Niño and neutral phases of ENSO. Moreover, these studies have only assessed relationships at the national scale, which may lead to the masking of ENSO relationships in (large) countries where ENSO and floods are oppositely correlated in different regions (e.g. Brazil, China, USA).

Finally, we discussed some important implications of these findings for future flood risk analyses and management. Additional research is needed to examine possible relationships between ENSO and flood impacts to supplement the current analysis of ENSO and flood discharges alone. Where such relationships exist, and the relationships are persistent through time, it could potentially be useful to combine this information with ongoing advances in ENSO predictability research, in order to provide probabilistic flood risk forecasts. This information may enable humanitarian and development agencies to prioritise short-term risk reduction efforts in the most at-risk regions, (re-)insurance companies to assess anomalies in their risk portfolios in the coming seasons to years, and may potentially enable improved flood early warning and flood regulation of dams.

Acknowledgements. This research was funded by a VENI grant from the Netherlands Organisation for Scientific Research (NWO). M. Kummu received funding from Aalto University Postdoc grants and the Academy of Finland funded project SCART (grant no. 267463). The financial support from the EU's Research Framework Programme (FP6) under contract no. 036946 (WATCH – Water and Global Change) is gratefully acknowledged. We acknowledge the Global Runoff Data Centre, Koblenz, Germany, for providing river discharge time series. We thank the editor, two anonymous reviewers, Hugo Hidalgo, and Gregory McCabe for their constructive comments on an earlier version of the manuscript.

Edited by: K. Stahl

Appendix A

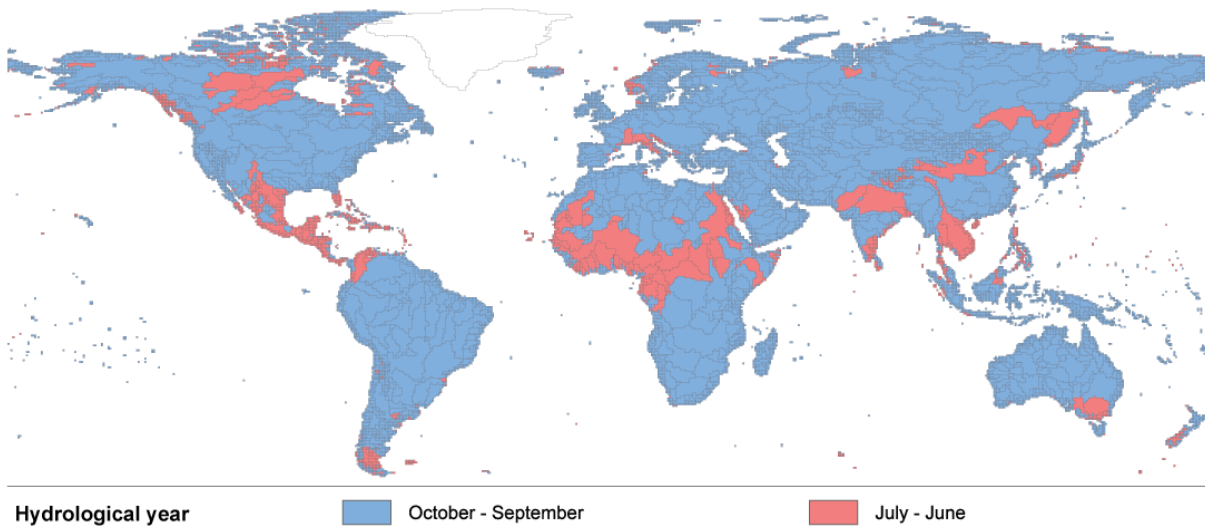


Fig. A1. Hydrological years used in this study for each basin. The standard hydrological year (October–September) was used as the default, except for in those basins in which the mean Q_{\max} of the most downstream cell occurs in the months of September, October, or November. In the latter case, the hydrological year was set to July–June.

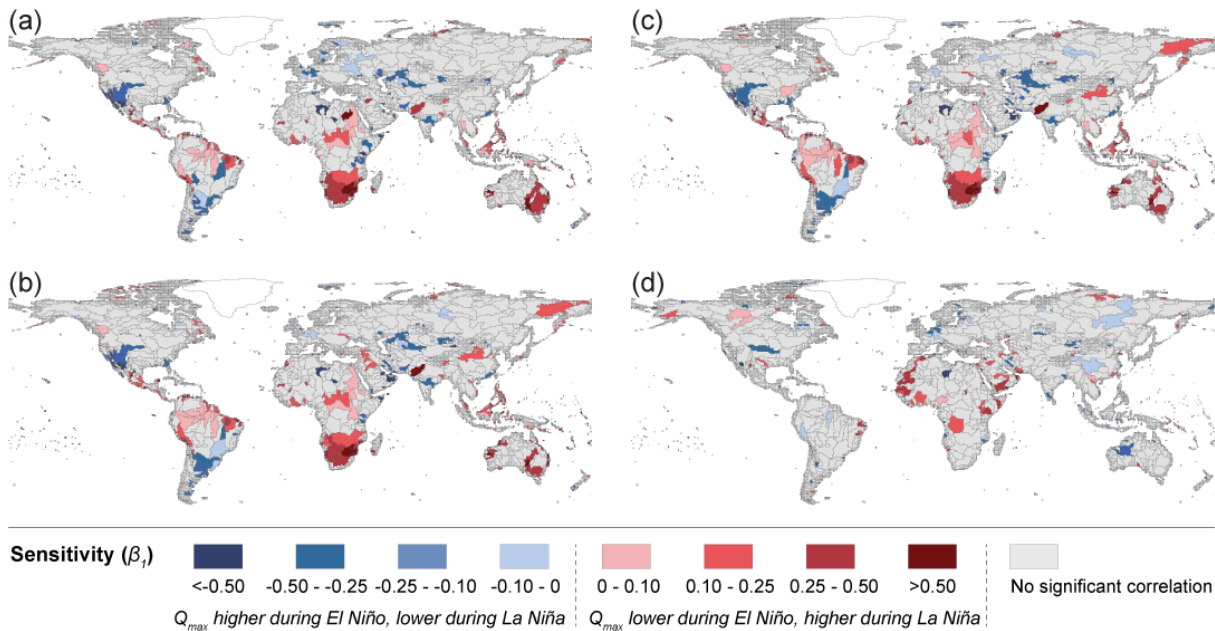


Fig. A2. Sensitivity (β) of $\ln Q_{\max}$ to variations in SOI for basins with significant correlation (Pearson’s r , t statistic, $\alpha = 0.10$). The sensitivity is shown for hydrological year Q_{\max} to 3-month mean SOI for (a) October–November–December (OND); (b) November–December–January (NDJ); (c) December–January–February (DJF); and (d) January–February–March (JFM). Negative correlation generally represents higher annual floods in El Niño years/lower annual floods in La Niña years, while positive correlation generally represents the opposite.

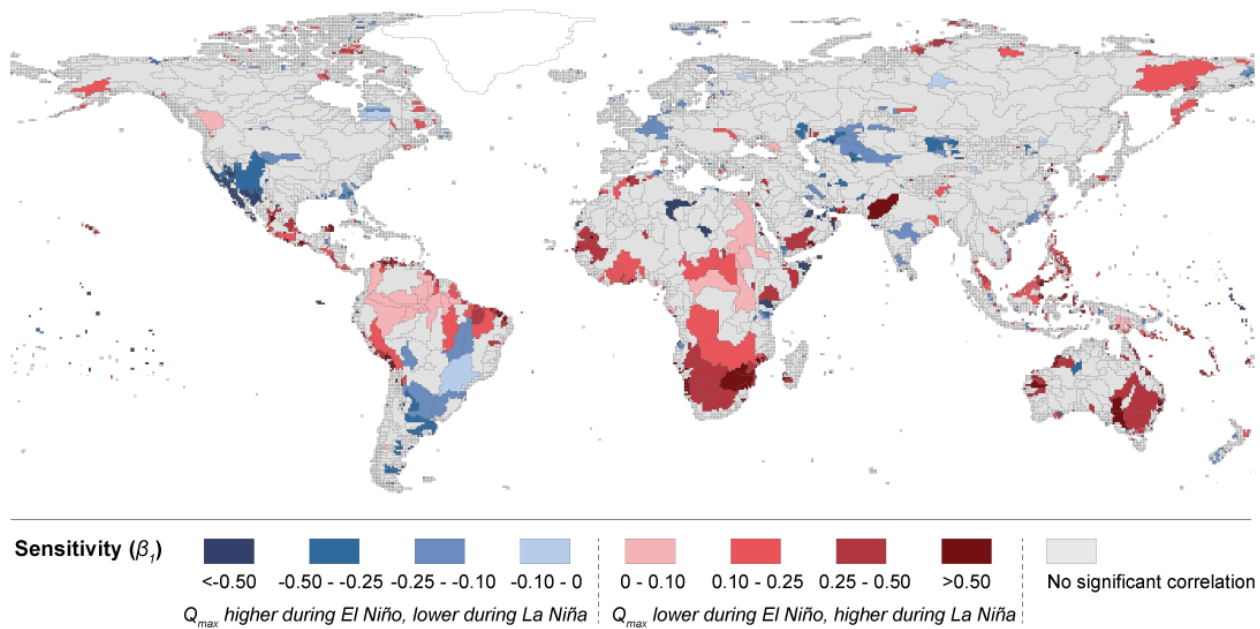


Fig. A3. Sensitivity (β_1) of $\ln Q_{\max}$ to variations in SOI. Sensitivity is only shown for basins with significant correlation at a 5% confidence interval (Pearson's r , t statistic, $\alpha = 0.05$). Negative correlation generally represents higher annual floods in El Niño years/lower annual floods in La Niña years, while positive correlation generally represents the opposite.

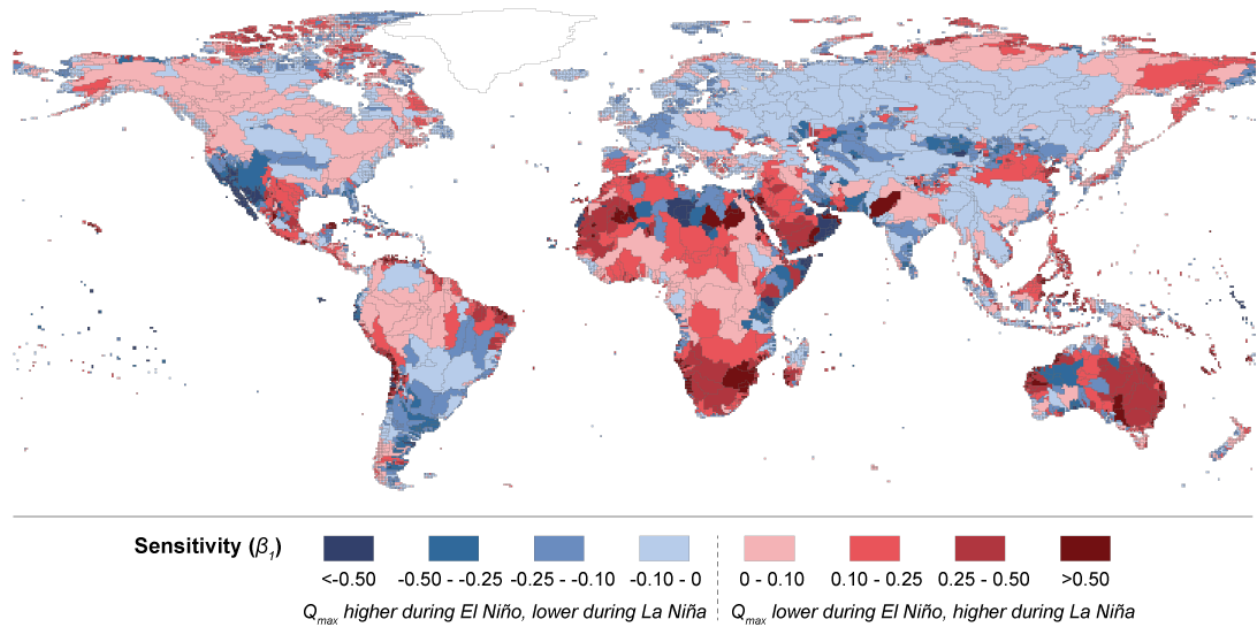


Fig. A4. Sensitivity (β_1) of $\ln Q_{\max}$ to variations in SOI. Negative correlation generally represents higher annual floods in El Niño years/lower annual floods in La Niña years, while positive correlation generally represents the opposite. For these results, no significance testing has been carried out.

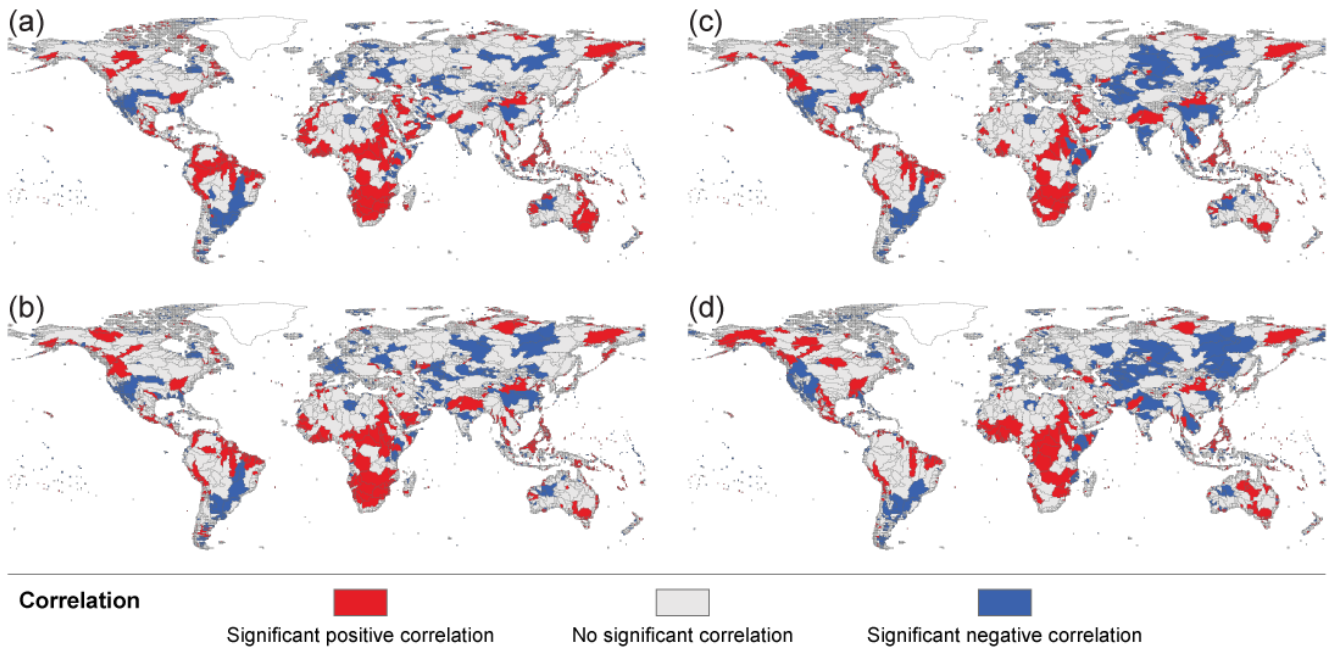


Fig. A5. Basins for which there is significant or no significant correlation between $\ln Q_{\max}$ and various indices of ENSO: (a) SOI; (b) inverse Multivariate ENSO Index (MEI); (c) inverse NINO3.4 index; and (d) inverse Global SST ENSO index. Statistical significance was tested using the t statistic ($\alpha = 0.10$).

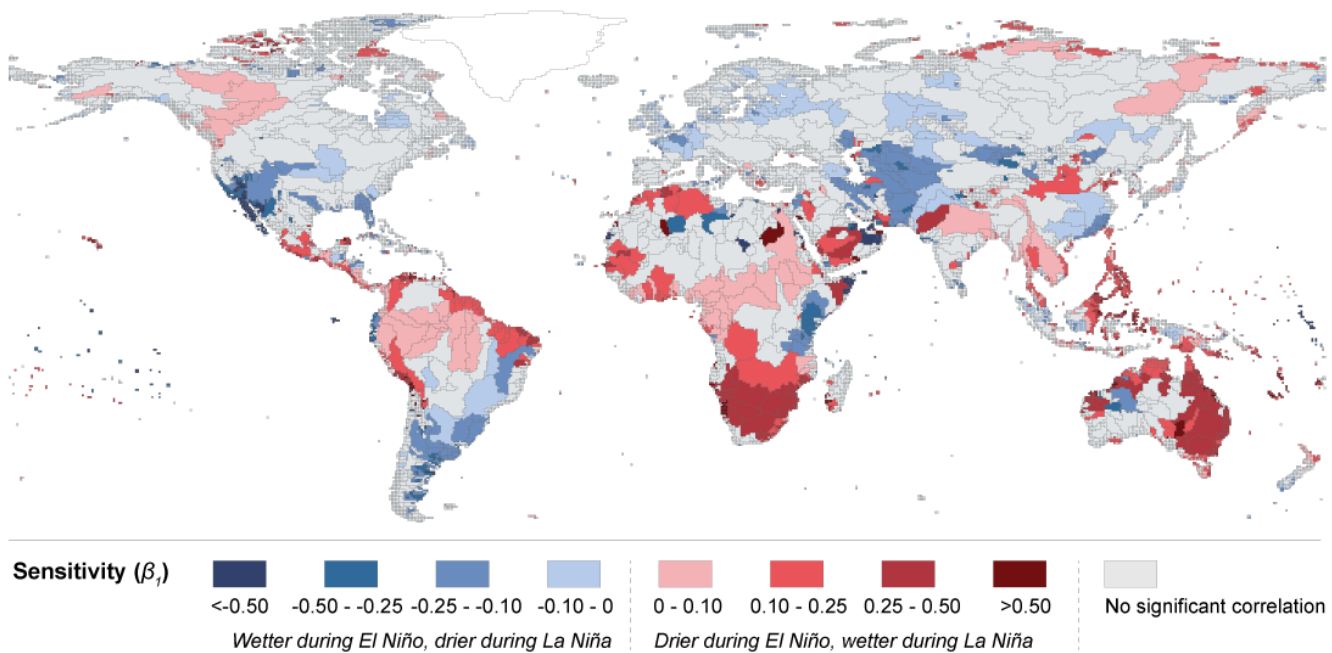


Fig. A6. Sensitivity (β_1) of $\ln Q_{\text{ann}}$ to variations in SOI (Pearson’s r , t statistic, $\alpha = 0.10$). Negative correlation generally represents wetter conditions in El Niño years/drier conditions in La Niña years, while positive correlation generally represents the opposite.

References

- Alcamo, J., Döll, P., Henrichs, T., Kaspar, F., Lehner, B., Rösch, T., and Siebert, S.: Development and testing of the WaterGAP2 global model of water use and availability, *Hydrolog. Sci. J.*, 48, 317–337, doi:10.1623/hysj.48.3.317.45290, 2003.
- Allamano, P., Claps, P., and Laio, F.: Global warming increases flood risk in mountainous areas, *Geophys. Res. Lett.*, 36, L24404, doi:10.1029/2009GL041395, 2009.
- Apipattanavis, S., McCabe, G. J., Rajagopalan, B., and Gangopadhyay, S.: Joint spatiotemporal variability of global sea surface temperatures and global Palmer Drought Severity Index values, *J. Climate*, 22, 6251–6267, doi:10.1175/2009JCLI2791.1, 2009.
- Beebee, R. A. and Manga, M.: Variation in the relationship between snowmelt runoff in Oregon and ENSO and PDO, *J. Am. Water Resour. Assoc.*, 40, 1011–1024, doi:10.1111/j.1752-1688.2004.tb01063.x, 2004.
- Bell, G. D. and Janowiak, J. E.: Atmospheric circulation associated with the Midwest Floods of 1993, *B. Am. Meteorol. Soc.*, 76, 681–695, doi:10.1175/1520-0477(1995)076<0681:ACAWTM>2.0.CO;2, 1995.
- Bouma, M. J., Kovats, R. S., Goubet, S.A., Cox, J. St. H., and Haines, A.: Global assessment of El Niño's disaster burden, *The Lancet*, 350, 1435–1438, doi:10.1016/S0140-6736(97)04509-1, 1997.
- Bouwer, L. M., Vermaat, J. E., and Aerts, J. C. J. H.: Regional sensitivities of mean and peak river discharge to climate variability in Europe, *J. Geophys. Res.*, 113, D19103, doi:10.1029/2008JD010301, 2008.
- Brown, C. and Lall, U.: Water and economic development: the role of variability and a framework for resilience, *Nat. Resour. Forum*, 30, 306–317, doi:10.1111/j.1477-8947.2006.00118.x, 2006.
- Cane, M. A.: The evolution of El Niño, past and future, *Earth Planet. Sc. Lett.*, 230, 227–240, doi:10.1016/j.epsl.2004.12.003, 2005.
- Cayan, D. R. and Webb, R. H.: El Niño/Southern Oscillation and streamflow in the western United States, in: *El Niño. Historical and paleoclimatic aspects of the Southern Oscillation*, edited by: Diaz, H. F. and Markgraf, V., Cambridge University Press, Cambridge, 29–68, 1992.
- Cayan, D. R., Redmond, K. T., and Riddle, L. G.: ENSO and hydrologic extremes in the western United States, *J. Climate*, 12, 2881–2893, doi:10.1175/1520-0442(1999)012<2881:EAHEIT>2.0.CO;2, 1999.
- Cheng, Y., Tang, Y., and Chen, D.: Relationship between predictability and forecast skill of ENSO on various time scales, *J. Geophys. Res.*, 116, C12006, doi:10.1029/2011JC007249, 2011.
- Chiew, F. H. S. and McMahon, T. A.: Global ENSO-streamflow teleconnection, streamflow forecasting and interannual variability, *Hydrolog. Sci. J.*, 47, 505–522, doi:10.1080/02626660209492950, 2002.
- Conway, D., Persechino, A., Ardoin-Bardin, S., Hamandawana, H., Dieulin, C., and Mahe, G.: Rainfall and water resources variability in sub-Saharan Africa during the twentieth century, *J. Hydrometeorol.*, 10, 41–59, doi:10.1175/2008JHM1004.1, 2009.
- Costanza, R., d'Arge, R., De Groot, R., Farber, S., Grasso, M., Hannon, B., Limburg, K., Naeem, S., O'Neil, R. V., Paruelo, J., Raskin, R. G., Sutton, P., and Van den Belt, M.: The value of the world's ecosystem services and natural capital, *Nature*, 387, 253–260, 1997.
- Cunderlik, J. M. and Ouarda, T. B. M. J.: Trends in the timing and magnitude of floods in Canada, *J. Hydrol.*, 375, 471–480, doi:10.1016/j.jhydrol.2009.06.050, 2009.
- Dankers, R. and Feyen, L.: Climate change impact on flood hazard in Europe: An assessment based on high-resolution climate simulations, *J. Geophys. Res.-Atmos.*, 113, D19105, doi:10.1029/2007JD009719, 2008.
- Dankers, R. and Feyen, L.: Flood hazard in Europe in an ensemble of regional climate scenarios, *J. Geophys. Res.-Atmos.*, 114, D16108, doi:10.1029/2008JD011523, 2009.
- Dettinger, M. D. and Diaz, H. F.: Global characteristics of stream flow seasonality and variability, *J. Hydrometeorol.*, 1, 289–310, doi:10.1175/1525-7541(2000)001<0289:GCOSFS>2.0.CO;2, 2000.
- Dettinger, M. D., Cayan, D. R., and McCabe, G. J.: Multiscale streamflow variability associated with El Niño/Southern Oscillation, in: *El Niño and the Southern Oscillation-Multiscale Variability and Global and Regional Impacts*, edited by: Diaz, H. F. and Markgraf, V., Cambridge University Press, Cambridge, 113–147, 2000.
- Dettinger, M. D., Battisti, D. S., Garreaud, R. D., McCabe, G. J., and Bitz, C. M.: Interhemispheric effects of interannual and decadal ENSO-like climate variations on the Americas, in: *Interhemispheric climate linkages: Present and Past Climates in the Americas and their Societal Effects*, edited by: Markgraf, V., Academic Press, San Diego, 1–16, 2001.
- Di Baldassarre, G., Montanari, A., Lins, H., Koutsoyiannis, D., Brandimarte, L., and Blöschl, G.: Flood fatalities in Africa: From diagnosis to mitigation, *Geophys. Res. Lett.*, 37, L22402, doi:10.1029/2010GL045467, 2010.
- Dilley, M. and Heyman, B. N.: ENSO and disaster: droughts, floods and El Niño/Southern Oscillation warm events, *Disasters*, 19, 181–193, 1995.
- Döll, P., Kaspar, F., and Lehner, B.: A global hydrological model for deriving water availability indicators: model tuning and validation, *J. Hydrol.*, 270, 105–134, doi:10.1016/S0022-1694(02)00283-4, 2003.
- Douglas, E. M., Vogel, R. M., and Kroll, C. N.: Trends in floods and low flows in the United States: impact of spatial correlation, *J. Hydrol.*, 240, 90–105, doi:10.1016/S0022-1694(00)00336-X, 2000.
- Feyen, L., Dankers, R., Bódis, K., Salamon, P., Barredo, J. I.: Fluvial flood risk in Europe in present and future climates, *Climatic Change*, 112, 47–62, doi:10.1007/s10584-011-0339-7, 2012.
- Gershunov, A. and Barnett, T. P.: Interdecadal modulation of ENSO teleconnections, *B. Am. Meteorol. Soc.*, 79, 2715–2725, doi:10.1175/1520-0477(1998)079<2715:IMOET>2.0.CO;2, 1998.
- Gershunov, A., Barnett, T. P., and Cayan, D. R.: North Pacific interdecadal oscillation seen as factor in ENSO-related North American climate anomalies, *EOS T. Am. Geophys. Un.*, 80, 25–30, doi:10.1029/99EO00019, 1999.
- Goddard, L. and Dilley, M.: El Niño: Catastrophe or opportunity, *J. Climate*, 18, 651–665, doi:10.1175/JCLI-3277.1, 2005.
- Gudmundsson, L., Tallaksen, L. M., Stahl, K., Clark, D. B., Dumont, E., Hagemann, S., Bertrand, N., Gerten, D., Heinke, J., Hanasaki, N., Voss, F., and Koiraala, S.: Comparing large-scale hydrological model simulations to observed runoff percentiles in

- Europe, *J. Hydrometeorol.*, 13, 604–620, doi:10.1175/JHM-D-11-083.1, 2011.
- Haddeland, I., Clark, D. B., Franssen, W., Ludwig, F., Voß, F., Arnell, N.W., Bertrand, N., Best, M., Folwell, S., Gerten, D., Gomes, S., Gosling, S. N., Hagemann, S., Hanasaki, N., Harding, R., Heinke, J., Kabat, P., Koirala, S., Oki, T., Polcher, J., Stacke, T., Viterbo, P., Weedon, G., and Yeh, P.: Multimodel estimate of the global terrestrial water balance: Setup and first results, *J. Hydrometeorol.*, 12, 869–884, doi:10.1175/2011JHM1324.1, 2011.
- Hannaford, J. and Marsh, T. J.: High-flow and flood trends in a network of undisturbed catchments in the UK, *Int. J. Climatol.*, 28, 1325–1338, doi:10.1002/joc.1643, 2008.
- Hidalgo, H. G. and Dracup, J. A.: ENSO and PDO effects on hydroclimatic variations of the Upper Colorado River Basin, *J. Hydrometeorol.*, 4, 5–23, doi:10.1175/1525-7541(2003)004<0005:EAPEOH>2.0.CO;2, 2003.
- Hirabayashi, Y., Kanae, S., Emori, S., Oki, T., and Kimoto, M.: Global projections of changing risks of floods and droughts in a changing climate, *Hydrolog. Sci. J.*, 53, 754–772, doi:10.1623/hysj.53.4.754, 2008.
- Hirabayashi, Y., Mahendran, R., Koirala, S., Konoshima, L., Yamazaki, D., Watanabe, S., Kim, H., and Kanae, S.: Global flood risk under climate change, *Nat. Clim. Change*, 3, 816–821, doi:10.1038/nclimate1911, 2013
- Hirsch, R. M. and Ryberg, K. R.: Has the magnitude of floods across the USA changed with global CO₂ levels?, *Hydrolog. Sci. J.*, 57, 1–9, doi:10.1080/02626667.2011.621895, 2012.
- Hoerling, M. P., Kumar, A., and Zhong, M.: El Niño, La Niña, and the nonlinearity of their teleconnections, *J. Climate*, 10, 1769–1786, doi:10.1175/1520-0442(1997)010<1769:ENOLNA>2.0.CO;2, 1997.
- Hoerling, M., Quan, X., and Eischeid, J.: Distinct causes for two principal U.S. droughts of the 20th century, *Geophys. Res. Lett.*, 36, L19708, doi:10.1029/2009GL039860, 2009.
- Hoerling, M., Eischeid, J., and Perlwitz, J.: Regional Precipitation Trends: Distinguishing Natural Variability from Anthropogenic Forcing, *J. Climate*, 23, 2131–2145, doi:10.1175/2009JCLI3420.1, 2010.
- IPCC: Managing the Risks of Extreme Events and Disasters to Advance Climate Change Adaptation. A Special Report of Working Groups I and II of the Intergovernmental Panel on Climate Change, Cambridge University Press, Cambridge, 2012.
- IPCC: Climate Change 2013: The Physical Science Basis—Summary for Policymakers. Draft report, IPCC-approved summary for policymakers, 36 p., http://www.climatechange2013.org/images/uploads/WGIAR5-SPM_Approved27Sep2013.pdf, 2013.
- Jongman, B., Ward, P. J., and Aerts, J. C. J. H.: Global exposure to river and coastal flooding – long term trends and changes, *Global Environ. Chang.*, 22, 823–835, doi:10.1016/j.gloenvcha.2012.07.004, 2012.
- Kiladis, G. N. and Diaz, H. F.: Global climatic anomalies associated with extremes in the Southern Oscillation, *J. Climatol.*, 2, 1069–1090, doi:10.1175/1520-0442(1989)002<1069:GCAAWE>2.0.CO;2, 1989.
- Kitoh, A., Kusunoki, S., and Nakaegawa, T.: Climate change projections over South America in the late 21st century with the 20 and 60 km mesh Meteorological Research Institute atmospheric general circulation model (MRIAGCM), *J. Geophys. Res.-Atmos.*, 116, D06105, doi:10.1029/2010JD014920, 2011.
- Kottek, M., Grieser, J., Beck, C., Rudolf, B., and Rubel, F.: World Map of the Köppen-Geiger climate classification updated, *Meteorol. Z.*, 15, 259–263, doi:10.1127/0941-2948/2006/0130, 2006.
- Kummu, M., Ward, P. J., De Moel, H., and Varis, O.: Is physical water scarcity a new phenomenon? Global assessment of water shortage over the last two millennia, *Environ. Res. Lett.*, 5, 034006, doi:10.1088/1748-9326/5/3/034006, 2010.
- Kundzewicz, Z. W., Mata, L. J., Arnell, N. W., Döll, P., Kabat, P., Jiménez, B., Miller, K.A., Oki, T., Sen, Z., and Shiklomanov, I. A.: in: *Climate Change 2007: Impacts, Adaptation and Vulnerability*, edited by: Parry, M. L., Canziani, O. F., Palutikof, J. P., Van der Linden, P. J., and Hanson, C. E., Cambridge University Press, Cambridge, UK, 173–210, 2007.
- Labat, D.: Cross wavelet analyses of annual continental freshwater discharge and selected climate indices, *J. Hydrol.*, 385, 269–278, doi:10.1016/j.jhydrol.2010.02.029, 2010.
- Lehner, B., Doll, P., Alcamo, J., Henrichs, T., and Kaspar, F.: Estimating the impact of global change on flood and drought risks in Europe: A continental, integrated analysis, *Clim. Change*, 75, 273–299, doi:10.1007/s10584-006-6338-4, 2006.
- Li, J., Xie, S.-P., Cook, E. R., Morales, M. S., Christie, D. A., Johnson, N. C., Chen, F., D’Arrigo, R., Fowler, A. M., Gou, X., and Fang, K.: El Niño modulations over the past seven centuries, *Nat. Clim. Change*, 3, 822–826, doi:10.1038/NCLIMATE1936, 2013.
- Mann, M. E., Park, J., and Bradley, R. S.: Global interdecadal and century-scale climate oscillations during the past five centuries, *Nature*, 378, 266–270, doi:10.1038/378266a0, 1995.
- Mann, M., Cane, M., Clement, A., and Zebiak, S. E.: Volcanic and solar forcing of El Niño over the past 1000 years, *J. Climate*, 18, 447–456, doi:10.1175/JCLI-3276.1, 2005.
- McCabe Jr., G. J. and Dettinger, M. D.: Decadal variations in the strength of ENSO teleconnections with precipitation in the western United States, *Int. J. Climatol.*, 19, 1399–1410, doi:10.1002/(SICI)1097-0088(199911)19:13<1399::AID-JOC457>3.0.CO;2-A, 1999.
- McCabe Jr., G. J., Palecki, M. A., and Betancourt, J. L.: Pacific and Atlantic influences on multidecadal drought frequency in the United States, *P. Natl. Acad. Sci. USA.*, 101, 4136–4141, doi:10.1073/pnas.0306738101, 2004.
- McPhaden, M. J., Zebiak, S. E., and Glantz, M. H.: ENSO as an integrating concept in Earth Science, *Science*, 314, 1740–1745, doi:10.1126/science.1132588, 2006.
- Meyers, G., McIntosh, P., Pigot, L., and Pook, M.: The years of El Niño, La Niña, and interactions with the tropical Indian ocean, *J. Climate*, 20, 2872–2880, doi:10.1175/JCLI4152.1, 2007.
- Milly, P. C. D., Wetherald, R. T., Dunne, K. A., and Delworth, T. L.: Increasing risk of great floods in a changing climate, *Nature*, 415, 514–517, doi:10.1038/415514a, 2002.
- Mirza, M. M. Q.: Climate change, flooding in South Asia and implications, *Reg. Environ. Change*, 11, S95–S107, doi:10.1007/s10113-010-0184-7, 2011.
- Mudelsee, M., Borngen, M., Tetzlaff, G., and Grunewald, U.: No upward trends in the occurrence of extreme floods in central Europe, *Nature*, 425, 166–169, doi:10.1038/nature01928, 2003.
- Mullan, A. B.: On the linearity and stability of Southern Oscillation-climate relationships for New Zealand. *Internat. J. Climatol.*, 15, 1365–1386, 1995.

- Munich Re: Topics Geo 2012 Issue. Natural Catastrophes 2011. Analyses, Assessments, Positions, Münchener Rückversicherungs-Gesellschaft, Munich, 2012.
- Neelin, J. D., Jin, F.-F., and Syu, H.-H.: Variations in ENSO phase locking, *J. Climate*, 13, 2570–2590, doi:10.1175/1520-0442(2000)013M2570:VIEPL>2.0.CO;2, 2000.
- Piechota, T. C. and Dracup, J. A.: Drought and regional hydrologic variation in the United States: associations with the El Niño–Southern Oscillation, *Water Resour. Res.*, 32, 1359–1373, doi:10.1029/96WR00353, 1996.
- Piechota, T. C., Dracup, J. A., and Fovell, R. G.: Western US streamflow and atmospheric circulation patterns during El Niño Southern Oscillation, *J. Hydrol.*, 201, 249–271, doi:10.1016/S0022-1694(97)00043-7, 1997.
- Power, S., Delage, F., Chung, C., Kociuba, G., and Keay, K.: Robust twenty-first-century projections of El Niño and related precipitation variability, *Nature*, 502, 541–545, doi:10.1038/nature12580, 2013.
- Prudhomme, C., Parry, S., Hannaford, J., and Clark, D. B.: How well do large-scale models reproduce regional hydrological extremes in Europe?, *J. Hydrometeorol.*, 12, 1181–1204, doi:10.1175/2011JHM1387.1, 2011.
- Räsänen, T. A. and Kumm, M.: Spatiotemporal influences of ENSO on precipitation and flood pulse in the Mekong Basin, *J. Hydrol.*, 476, 154–168, doi:10.1016/j.jhydrol.2012.10.028, 2013.
- Redmond, K. T. and Koch, R. W.: Surface climate and streamflow variability in the Western United States and their relationship to large-scale circulation indices, *Water Resour. Res.*, 27, 2381–2399, doi:10.1029/91WR00690, 1991.
- Shiklomanov, A. I., Lammers, R. B., Rawlins, M. A., Smith, L. C., and Pavelsky, T. M.: Temporal and spatial variations in maximum river discharge from a new Russian data set, *J. Geophys. Res.*, 112, G04S53, doi:10.1029/2006JG000352, 2007.
- Torrence, C. and Webster, P. J.: Interdecadal Changes in the ENSO–Monsoon System, *J. Climate*, 12, 2679–2690, doi:10.1175/1520-0442(1999)012<2679:ICITEM>2.0.CO;2, 1999.
- Tudhope, A. W., Chilcott, C. P., McCulloch, M. T., Cook, E. R., Chappell, J., Ellam, R. M., Lea, D. W., Lough, J. M., and Shimmield, G. B.: Variability in the El Niño–Southern Oscillation Through a Glacial–Interglacial Cycle, *Science*, 291, 1511–1517, doi:10.1126/science.1057969, 2001.
- Ummenhofer, C. C., England, M. H., McIntosh, P. C., Meyers, G. A., Pook, M. J., Risbey, J. S., Gupta, A. S., and Taschetto, A. S.: What causes southeast Australia’s worst droughts?, *Geophys. Res. Lett.*, 36, L04706, doi:10.1029/2008GL036801, 2009.
- UNISDR: Global Assessment Report on Disaster Risk Reduction. Revealing Risk, Redefining Development, United Nations International Strategy for Disaster Reduction Secretariat, Geneva, 2011.
- Uppala, S. M., Kallberg, P. W., Simmons, A. J., Andrae, U., Da Costa Bechtold, V., Fiorino, M., Gibson, J. K., Haseler, J., Hernandez, A., Kelly, G. A., Li, X., Onogi, K., Saarinen, S., Sokka, N., Allan, R. P., Andersson, E., Arpe, K., Balmaseda, M. A., Beljaars, A. C. M., Van De Berg, L., Bidlot, J., Bormann, N., Caires, S., Chevallier, F., Dethof, A., Dragosavac, M., Fisher, M., Fuentes, M., Hagemann, S., Holm, E., Hoskins, B. J., Isaksen, I., Janssen, P., Jenne, R., McNally, A. P., Mahfouf, J.-F., Morcrette, J.-J., Rayner, N. A., Saunders, R. W., Simon, P., Serf, A., Trenberth, K. E., Untch, A., Vasiljevic, D., Viterbo, P., and Woolen, J.: The ERA-40 re-analysis, *Q. J. Roy. Meteor. Soc.*, 131B, 2961–3012, doi:10.1256/qj.04.176, 2005.
- Villarini, G. and Smith, J. A.: Flood peak distributions for the Eastern United States, *Water Resour. Res.*, 46, W06504, doi:10.1029/2009WR008395, 2010.
- Villarini, G., Serinaldi, F., Smith, J. A., and Krajewski, W. F.: On the stationarity of annual flood peaks in the continental United States during the 20th century, *Water Resour. Res.*, 45, W08417, doi:10.1029/2008WR007645, 2009.
- Wang, B., Yang, J., Zhou, T., and Wang, B.: Inter-decadal changes in the major modes of Asian–Australian monsoon variability: Strengthening relationship with ENSO since the late 1970s, *J. Climate*, 21, 1771–1789, doi:10.1175/2007JCLI1981.1, 2008.
- Ward, P. J., Beets, W., Bouwer, L. M., Aerts, J. C. J. H., and Renssen, H.: Sensitivity of river discharge to ENSO, *Geophys. Res. Lett.*, 37, L12402, doi:10.1029/2010GL043215, 2010.
- Ward, P. J., Jongman, B., Sperna Weiland, F., Bouwman, A., Van Beek, R., Bierkens, M., Ligtoet, W., and Winsemius, H.: Assessing flood risk at the global scale: model setup, results, and sensitivity, *Environ. Res. Lett.*, 8, 044019, doi:10.1088/1748-9326/8/4/044019, 2013.
- Waylen, P. R. and Caviedes, C. N.: El Niño and annual floods on the north Peruvian littoral, *J. Hydrol.*, 89, 141–156, doi:10.1016/0022-1694(86)90148-4, 1986.
- Weedon, G. P., Gomes, S., Viterbo, P., Shuttleworth, W. J., Blyth, E., Österle, H., Adam, J. C., Bellouin, N., Boucher, O., and Best, M.: Creation of the WATCH forcing data and its use to assess global and regional reference crop evaporation over land during the twentieth century, *J. Hydrometeorol.*, 12, 823–848, doi:10.1175/2011JHM1369.1, 2011.
- Wunsch, C.: The Interpretation of Short Climate Records, with Comments on the North Atlantic and Southern Oscillations, *B. Am. Meteorol. Soc.*, 80, 245–255, doi:10.1175/1520-0477(1999)080<0245:TIOSCR>2.0.CO;2, 1999.
- Zubair, L. and Chandimala, J.: Epochal Changes in ENSO–Streamflow Relationships in Sri Lanka, *J. Hydrometeorol.*, 7, 1237–1246, doi:10.1175/JHM546.1, 2006.